AIMS Mathematics, 10(8): 19512–19539.
DOI: 10.3934/math.2025871
Received: 01 June 2025
Revised: 25 July 2025
Accepted: 06 August 2025
Published: 26 August 2025

https://www.aimspress.com/journal/Math

Research article

Chemo-immunotherapy for optimal control of Tumor using Hilfer fractional derivative

K. Ramalakshmi[1], B. Sundara Vadivoo[2], Dilber Uzun Ozsahin[3,4,5], Hijaz Ahmad[5,6,*] and Taha Radwan[7,*]

[1] Department of Mathematics, Alagappa University, Karaikudi-630 004, India

[2] Department of Mathematics, Central University of Tamil Nadu, Thiruvarur-610 005, India

[3] Department of Medical Diagnostic Imaging, College of Health Sciences, University of Sharjah, UAE

[4] Research Institute for Medical and Health Sciences, University of Sharjah, UAE

[5] Operational Research Center in Healthcare, Near East University, Nicosia/TRNC, 99138 Mersin 10, Turkey

[6] Department of Mathematics, College of Science, Korea University, 145 Anam-ro, Seongbuk-gu, Seoul 02841, South Korea

[7] Department of Management Information Systems, College of Business and Economics, Qassim University, Buraydah 51452, Saudi Arabia

* **Correspondence:** Email: hijaz.ahmad@neu.edu.tr, t.radwan@qu.edu.sa.

Abstract: This research investigated an optimal control problem formulated using a Hilfer fractional-order differential model to describe the dynamics between tumor cells and the immune system during immuno-chemotherapy. The model emphasized the activation timing of effector cells and their capacity to generate a potent immune response against the tumor. The primary objective was to minimize the costs associated with immuno-chemotherapy while simultaneously reducing the tumor cell population through optimal control strategies. By solving both the state and adjoint equations, the optimal control problem was addressed numerically. Simulation results demonstrated that the proposed immuno-chemotherapy protocol significantly reduced the tumor burden.

Keywords: oncology; chemotherapy; immunotherapy; optimal control; fractional derivatives
Mathematics Subject Classification: 26A33, 49K05, 92C50

1. Introduction

Cancer remains a leading cause of death worldwide, affecting populations in both developed and developing nations. Despite significant advancements in understanding the interactions between tumor cells and the immune system, the effective treatment of cancer continues to be one of the most formidable challenges in contemporary medicine. The overarching goal of cancer treatment is to eradicate tumor cells while preserving a healthy proportion of the body's normal cells. Although chemotherapy is a cornerstone of cancer treatment, it does not always guarantee the complete elimination of tumor cells. Recently, immunotherapy has emerged as a promising complementary approach, demonstrating remarkable progress in enhancing the immune system's natural ability to target and destroy cancer cells [1–3].

Immunotherapy has become an integral component of modern cancer treatment, with particular emphasis on aAdoptive cellular immunotherapy (ACI). ACI enhances or restores the immune system's ability to combat cancer, typically utilizing cytokines that are either harvested from the patient's body or produced synthetically. These cytokines stimulate and support the immune system, enhancing its capacity to fight cancer. Although the exact mechanisms of immunotherapy are not yet fully understood, it is believed to slow or halt the growth of cancer cells, prevent metastasis, and strengthen the immune system's ability to eliminate tumor cells [4–6].

In contrast to traditional chemotherapy, which directly targets and destroys tumor cells, Interleukin-2 (IL-2) functions primarily by activating immune cells, such as T-cells and natural killer (NK) cells. Once activated, these immune cells can recognize and destroy cancer cells upon contact. ACI involves collecting T-cells from the patient, expanding them in the laboratory, and reintroducing them into the patient's body, thereby enhancing the immune response against cancer [1, 2].

In addition to surgery, chemotherapy and radiation therapy are conventional treatment modalities for cancer. Chemotherapy targets rapidly dividing cancer cells, aiming to eliminate them more quickly than normal cells, while radiation therapy employs high-energy rays to achieve similar outcomes. In certain cases, immunotherapy is administered either as a standalone treatment or as maintenance therapy following chemotherapy or radiation therapy. However, these treatments are often associated with significant side effects, including damage to healthy cells and suppression of the immune system, thereby increasing patients' susceptibility to infections. Consequently, restoring or enhancing the immune system after chemotherapy-induced depletion becomes crucial for the effectiveness of cancer treatment. Strengthening the body's natural defenses alongside chemotherapy offers a more promising strategy for combating cancer. The primary challenge, however, lies in determining the most effective approach to integrating chemotherapy with immunotherapy to achieve optimal outcomes for patients [7, 8].

The interactions between tumor cells and the immune system are complex and multifaceted, necessitating advanced modeling techniques to accurately capture their dynamics. Mathematical models have emerged as valuable tools for studying these interactions over time. A foundational model comprising a system of three ordinary differential equations (ODEs) was first proposed by Kirschner and Panetta [9]. Since then, numerous studies have extended these models to incorporate interactions between tumor cells and immune cells, normal cells, and the effects of chemotherapy.

Recently, fractional calculus has gained considerable attention due to its capability to model

complex systems across various disciplines, including biology, medicine, hydrology, finance, and engineering [10]. Although fractional differential equations (FDEs) have been extensively studied within biological contexts, there remains limited research on integrating them with optimal control theory for cancer treatment [11–14].

This study aims to develop, analyze, and computationally investigate optimal strategies for combining immunotherapy and chemotherapy in cancer treatment. The objective is to devise an optimal treatment plan that reduces tumor size while enhancing immune system functionality and minimizing side effects for the patient. Utilizing Hilfer derivatives [15–17], we construct a fractional differential model to describe the tumor-immune system dynamics under various treatment regimens, including immunotherapy and chemotherapy.

The use of Hilfer derivatives is particularly advantageous in this context, as they provide a more nuanced representation of biological processes such as T-cell activation and IL-2 production, which are central to the immune response. Furthermore, we formulate an optimal control problem to determine the best set of control variables and optimize the treatment strategy.

The primary contributions of this study are as follows:

- Development of a fractional differential model that integrates both chemotherapy and immunotherapy, employing Hilfer derivatives to more accurately capture the dynamics of tumor–immune interactions.
- Formulation of an optimal control problem aimed at minimizing the tumor cell population and chemotherapy costs while enhancing immune responses, thereby providing an effective strategy for cancer treatment.
- Application of Pontryagin's Maximum Principle to derive the necessary optimality conditions for the control problem, offering a systematic framework for determining optimal treatment strategies.
- Numerical validation of the proposed model and control strategy, demonstrating the effectiveness of immuno-chemotherapy in reducing tumor burden while minimizing side effects.

1.1. Motivation of the model

Cancer remains a leading cause of mortality worldwide, necessitating effective treatment strategies that can manage tumor growth while minimizing adverse effects. Chemotherapy is widely used to reduce tumor burden by directly killing rapidly dividing cancer cells, whereas immunotherapy enhances the body's immune response to target and eliminate tumor cells. Combining these therapies, known as chemo-immunotherapy, leverages their complementary effects to achieve better treatment outcomes. However, designing effective combined treatment protocols requires a deep understanding of the dynamic interactions among tumor cells, immune responses, and drug effects over time. Traditional integer-order models often fail to capture the memory and hereditary properties inherent in biological processes. In this context, fractional-order derivatives, particularly the Hilfer fractional derivative, provide a flexible framework to model these memory effects while interpolating between the Riemann–Liouville and Caputo derivatives. The motivation behind developing the proposed model is to utilize the Hilfer fractional derivative within an optimal control framework to design and analyze chemo-immunotherapy protocols that can effectively reduce tumor size, preserve immune response, and minimize drug dosage, thereby providing practical insights for improving cancer treatment strategies.

1.2. Organization of the paper

The structure of this study is organized as follows:

- Section 2 introduces the key concepts of fractional calculus, including the definitions and properties of the Hilfer fractional derivative relevant to modeling biological memory effects.
- Section 3 presents the mathematical model describing the interactions between tumor cells and the immune system under chemotherapy and immunotherapy (including ACI and IL-2), formulated as a system of Hilfer fractional differential equations.
- Section 4 analyzes the stability of steady states, focusing on stability in the absence of treatment, under therapeutic interventions, and the biological interpretation of the stability results.
- Section 5 addresses the optimal control problem, discussing the existence and uniqueness of optimal controls using the Banach fixed-point theorem and deriving necessary conditions for optimality via Pontryagin's Maximum Principle, along with numerical methods to compute optimal controls.
- Section 6 presents numerical simulations to validate the theoretical results and illustrate the effectiveness of the proposed chemo-immunotherapy treatment strategies under different fractional orders and parameter scenarios.
- Section 7 concludes the study and outlines potential directions for future research, including parameter estimation using real data and extension of the model to more complex tumor-immune dynamics.

2. Preliminaries

Fractional-order derivatives can be defined through various approaches, among which the Caputo and Riemann–Liouville definitions are the most commonly utilized. The Hilfer fractional derivative, a generalization of the classical Riemann–Liouville derivative [15], offers enhanced flexibility for modeling physical and biological phenomena, making it well-suited for capturing memory and hereditary properties inherent in many real-world systems. Notably, the Hilfer derivative allows interpolation between the Caputo and Riemann–Liouville derivatives through its type parameter, providing additional degrees of freedom that enable more accurate representation of complex dynamic behaviors in biological models, including cancer-immune system interactions.

Definition 2.1. *[10] The fractional integral of order $\alpha > 0$ with the lower limit a for a function $\varphi : [a, \infty) \to \mathbb{R}$ is given by*

$$\mathcal{I}^{\alpha}_{a+}\varphi(x) = \frac{1}{\Gamma(\alpha)} \int_a^x \frac{\varphi(\varsigma)}{(x-\varsigma)^{1-\alpha}} d\varsigma, \quad x > a, \quad \alpha > 0.$$

Definition 2.2. *[10] The Riemann-Liouville derivative of order $\alpha > 0$ for a function $\varphi : [a, \infty) \to \mathbb{R}$ is defined as*

$$\mathcal{D}^{\alpha}_{a+}\varphi(x) = \frac{1}{\Gamma(n-\alpha)} \left(\frac{d}{dx}\right)^n \int_a^x \frac{\varphi(\varsigma)}{(x-\varsigma)^{1-n+\alpha}} d\varsigma, \quad x > a, \quad n-1 < \alpha < n.$$

Definition 2.3. *[10] The Caputo fractional derivative of order $\alpha > 0$ is expressed as*

$${}^{C}\mathcal{D}^{\alpha}_{a+}\varphi(x) = \frac{1}{\Gamma(n-\alpha)} \int_a^x (x-t)^{n-\alpha-1} \varphi^{(n)}(\varsigma) dt, \quad n-1 < \alpha < n.$$

Definition 2.4. *[15] The Hilfer fractional derivative, also known as the generalized Riemann–Liouville derivative, of order $n-1 < \alpha < n$ and $0 < \beta < 1$ is defined as:*

$$ {}^{\mathcal{H}}\mathcal{D}_{a+}^{\alpha,\beta}\varphi(x) = \mathcal{I}_{a+}^{\beta(n-\alpha)}\frac{d}{dx}\mathcal{I}_{a+}^{(n-\alpha)(1-\beta)}\varphi(x). $$

Theorem 2.5. *Consider the system*

$$ {}^{\mathcal{H}}\mathcal{D}_{a+}^{\alpha,\beta}\varphi(x) = \varphi(\varsigma, \mathcal{Z}(\varsigma)), \quad \mathcal{Z}(\varsigma_0) = \mathcal{Z}_0. $$

Let $\mathcal{J}(\mathcal{Z}^*)$ represent the Jacobian matrix of the system at the equilibrium point $\mathcal{Z}^*$. The stability of the equilibrium point $\mathcal{Z}^*$ is characterized as follows:

(1) The equilibrium point $\mathcal{Z}^*$ is locally asymptotically stable if, and only if, all eigenvalues ϕ_i, $i = 1, 2, \ldots, n$, of $\mathcal{J}(\mathcal{Z}^*)$ satisfy $|\arg(\phi_i)| > \frac{\alpha\pi}{2}$.

(2) The equilibrium point $\mathcal{Z}^*$ is stable if all eigenvalues ϕ_i, $i = 1, 2, \ldots, n$, of $\mathcal{J}(\mathcal{Z}^*)$ satisfy $|\arg(\phi_i)| \geq \frac{\alpha\pi}{2}$, and eigenvalues with $|\arg(\phi_i)| = \frac{\alpha\pi}{2}$ have the same geometric and algebraic multiplicity.

(3) The equilibrium point $\mathcal{Z}^*$ is unstable if, and only if, there exists an eigenvalue ϕ_i, for some $i = 1, 2, \ldots, n$, of $\mathcal{J}(\mathcal{Z}^*)$ such that $|\arg(\phi_i)| < \frac{\alpha\pi}{2}$.

Theorem 2.6. *(Banach fixed-point theorem) Let X be a nonempty Banach space equipped with a norm $\|\cdot\|$, and let $T : X \to X$ be a contraction mapping; that is, there exists a constant $0 \leq k < 1$ such that*

$$ \|T(x) - T(y)\| \leq k\,\|x - y\| $$

for all $x, y \in X$. Then

- *T has a unique fixed point $x^* \in X$ such that $T(x^*) = x^*$.*
- *For any initial point $x_0 \in X$, the sequence defined by*

$$ x_{n+1} = T(x_n), \quad n = 0, 1, 2, \ldots $$

  converges to x^*.
- *The following estimate holds*

$$ \|x_n - x^*\| \leq \frac{k^n}{1-k}\|x_0 - x_1\|. $$

Remark. The Banach fixed-point theorem is used in this paper to prove the existence and uniqueness of solutions for the Hilfer fractional-order optimal control system. By defining a suitable Banach space of continuous functions on a closed interval with the supremum norm and constructing an appropriate contraction mapping derived from the equivalent integral form of the Hilfer fractional system, we apply this theorem to ensure that the system admits a unique solution under the assumptions specified.

3. Model description

In this section, we develop a mathematical model of tumor-immune interactions, incorporating different populations of immune and tumor cell types. The dynamics of how certain immunogenic tumors evade typical immune surveillance are explored by analyzing the interaction between effector

cells and tumor cells. The model includes five time-dependent variables, with two control variables, $v(\varsigma)$ and $w(\varsigma)$, used to assess the effects of immunotherapy and chemotherapy. The key variables of the model are described as follows (Table 1):

Table 1. Model variables.

Variable	Description
$\mathbb{E}(\varsigma)$	Effector cells
$\mathbb{T}(\varsigma)$	Tumor cells
$\mathbb{I}(\varsigma)$	Concentration of Interleukin-2 in a single tumor site compartment
$\mathbb{N}(\varsigma)$	Normal cells
$\mathbb{U}(\varsigma)$	Amount of drugs in chemotherapy

The parameters of the model are detailed in [9]. The new system is modeled using Hilfer fractional-order differential equations as outlined below:

$$
\begin{aligned}
{}^{\mathcal{H}}\mathcal{D}_{0+}^{\alpha,\beta}\mathbb{E}(\varsigma) &= \zeta^{\alpha,\beta}\mathbb{T}(\varsigma) - \mu_1^{\alpha,\beta}\mathbb{E}(\varsigma) + g_1^{\alpha,\beta}\mathbb{E}(\varsigma)\mathbb{I}(\varsigma) + w(\varsigma)s_1^{\alpha,\beta} - \gamma_1^{\alpha,\beta}(1-e^{-\mathbb{U}(\varsigma)})\mathbb{E}(\varsigma), && (3.1)\\
{}^{\mathcal{H}}\mathcal{D}_{0+}^{\alpha,\beta}\mathbb{T}(\varsigma) &= a_1^{\alpha,\beta}\mathbb{T}(\varsigma)(1-b_1\mathbb{T}(\varsigma)) - g_2^{\alpha,\beta}\mathbb{E}(\varsigma)\mathbb{T}(\varsigma) - \eta_1^{\alpha,\beta}\mathbb{N}(\varsigma)\mathbb{T}(\varsigma)\\
&\quad -\gamma_2^{\alpha,\beta}(1-e^{-\mathbb{U}(\varsigma)})\mathbb{T}(\varsigma), && (3.2)\\
{}^{\mathcal{H}}\mathcal{D}_{0+}^{\alpha,\beta}\mathbb{I}(\varsigma) &= g_3^{\alpha,\beta}\mathbb{E}(\varsigma)\mathbb{T}(\varsigma) - \mu_2^{\alpha,\beta}\mathbb{I}(\varsigma) + s_2^{\alpha,\beta}, && (3.3)\\
{}^{\mathcal{H}}\mathcal{D}_{0+}^{\alpha,\beta}\mathbb{N}(\varsigma) &= a_2^{\alpha,\beta}\mathbb{N}(\varsigma)(1-b_2\mathbb{N}(\varsigma)) - \eta_2^{\alpha,\beta}\mathbb{T}(\varsigma)\mathbb{N}(\varsigma) - \gamma_3^{\alpha,\beta}(1-e^{-\mathbb{U}(\varsigma)})\mathbb{N}(\varsigma), && (3.4)\\
{}^{\mathcal{H}}\mathcal{D}_{0+}^{\alpha,\beta}\mathbb{U}(\varsigma) &= v(\varsigma) - d^{\alpha,\beta}\mathbb{U}(\varsigma). && (3.5)
\end{aligned}
$$

The first equation captures the fractional-order dynamics of effector immune cells under treatment interventions. Biologically, effector cells are critical for identifying and destroying tumor cells, and their dynamics are influenced by tumor presence, cytokines, and treatment interventions. The term $\zeta^{\alpha,\beta}\mathbb{T}(\varsigma)$ represents the stimulation of effector cells in response to tumor antigens, indicating how the immune system becomes activated when tumors are present. The natural death of effector cells over time is modeled by $-\mu_1^{\alpha,\beta}\mathbb{E}(\varsigma)$. The interaction between IL-2 and effector cells, which boosts effector proliferation, is described by $g_1^{\alpha,\beta}\mathbb{E}(\varsigma)\mathbb{I}(\varsigma)$. The term $w(\varsigma)s_1^{\alpha,\beta}$ represents the effect of administered immunotherapy, such as adoptive cellular immunotherapy or external cytokine infusion, enhancing the effector cell count. Finally, the impact of chemotherapy on effector cells is expressed through $-\gamma_1^{\alpha,\beta}(1-e^{-\mathbb{U}(\varsigma)})\mathbb{E}(\varsigma)$, illustrating how chemotherapy can damage immune cells, with a saturating response that realistically captures drug cytotoxicity. Mathematically, this equation leverages the Hilfer fractional derivative to capture the system's memory and hereditary effects, providing a refined representation of immune cell dynamics over time under treatment.

The second equation governs the behavior of tumor cells in the system, accounting for their proliferation, death due to immune activity, and the effects of chemotherapy. Tumor cells exhibit logistic growth, modeled by $a_1^{\alpha,\beta}\mathbb{T}(\varsigma)(1-b_1\mathbb{T}(\varsigma))$, where $a_1^{\alpha,\beta}$ is the growth rate and b_1 captures the tumor's carrying capacity within the biological environment. The immune system's suppression of tumor cells is represented by the term $-g_2^{\alpha,\beta}\mathbb{E}(\varsigma)\mathbb{T}(\varsigma)$, reflecting the cytotoxic action of effector cells on tumor cells. Additionally, the inhibitory role of normal cells in suppressing tumor proliferation is described by $-\eta_1^{\alpha,\beta}\mathbb{N}(\varsigma)\mathbb{T}(\varsigma)$, indicating competition for space and resources within the tissue

environment. The chemotherapy-induced death of tumor cells is captured by $-\gamma_2^{\alpha,\beta}(1 - e^{-\mathbb{U}(\varsigma)})\mathbb{T}(\varsigma)$, incorporating drug saturation effects for realistic modeling. Using Hilfer fractional derivatives allows this equation to incorporate memory effects in tumor proliferation and response to treatment, which is crucial in capturing the delayed and history-dependent behavior seen in real tumor growth and therapy response.

The third equation models the fractional-order dynamics of IL-2, a cytokine essential for activating and sustaining immune responses against tumors. IL-2 is produced when effector cells interact with tumor cells, modeled by $g_3^{\alpha,\beta}\mathbb{E}(\varsigma)\mathbb{T}(\varsigma)$, which represents immune system activation in response to the tumor presence. Natural degradation and clearance of IL-2 from the system are described by $-\mu_2^{\alpha,\beta}\mathbb{I}(\varsigma)$, reflecting its limited half-life in the body. Additionally, $s_2^{\alpha,\beta}$ denotes a constant source of IL-2, which could be due to baseline physiological production or external therapeutic administration to support immune function. The use of the Hilfer fractional derivative in this equation facilitates capturing the nonlocal and history-dependent dynamics of IL-2 kinetics, which is essential for accurately modeling its transient yet critical role in immune activation during cancer therapy.

The fourth equation addresses the dynamics of normal (healthy) cells within the system, considering their growth, competition with tumor cells, and damage due to chemotherapy. Normal cells undergo logistic growth described by $a_2^{\alpha,\beta}\mathbb{N}(\varsigma)(1 - b_2\mathbb{N}(\varsigma))$, reflecting their proliferation constrained by the tissue environment's carrying capacity. The suppressive influence of tumor cells on normal cells, which often occurs due to the invasive behavior of cancer, is modeled by $-\eta_2^{\alpha,\beta}\mathbb{T}(\varsigma)\mathbb{N}(\varsigma)$. Additionally, the cytotoxic effects of chemotherapy on normal cells are captured by $-\gamma_3^{\alpha,\beta}(1 - e^{-\mathbb{U}(\varsigma)})\mathbb{N}(\varsigma)$, indicating the nonselective nature of many chemotherapeutic agents that harm both tumor and normal cells. By employing the Hilfer fractional derivative, this equation captures the memory effects in normal cell regeneration and damage, which is crucial in reflecting the biological delays observed in recovery and depletion due to chemotherapy during cancer treatment.

The fifth equation models the pharmacokinetics of the chemotherapy drug within the body under fractional-order dynamics. The control variable $v(\varsigma)$ represents the administration rate of the chemotherapeutic agent, which can be adjusted as part of the treatment strategy. The drug's clearance from the body is represented by the term $-d^{\alpha,\beta}\mathbb{U}(\varsigma)$, where $d^{\alpha,\beta}$ denotes the fractional clearance rate, capturing the elimination of the drug over time. By using the Hilfer fractional derivative, this equation accounts for memory-dependent drug kinetics, reflecting how chemotherapy may persist and accumulate in tissues, influencing treatment efficacy and toxicity over time. This component is critical in designing optimal control strategies that balance effective tumor suppression with the minimization of adverse effects on the immune system and normal tissues.

The details of the parameters are as follows (Table 2).

Table 2. Model parameters for tumor with immuno-chemotherapy and their values.

Parameter	Definition	Values
ζ	Tumor antigenicity rate	$0.103\,\text{day}^{-1}$
μ_1	Natural degradation rate of effector cells	$0.08\,\text{day}^{-1}$
μ_2	Natural degradation rate of IL-2	$20\,\text{day}^{-1}$
g_1	Proliferation rate of effector cells	$1\,\text{cell}^{-1}\,\text{day}^{-1}$
g_2	Tumor cell decay rate	$1.8\,\text{day}^{-1}$
g_3	Growth rate of IL-2	$1\,\text{day}^{-1}$
$s_i (i = 1, 2)$	Exogenous treatment factors	$[0, 40]\,\text{day}^{-1}$
γ_1	Chemotherapy-induced effector cell mortality rate	$0.65\,\text{day}^{-1}$
γ_2	Chemotherapy-induced tumor cell mortality rate	$0.45\,\text{day}^{-1}$
γ_3	Chemotherapy-induced normal cell mortality rate	$0.02\,\text{day}^{-1}$
a_1	Tumor cell growth rate	$0.28\,\text{day}^{-1}$
a_2	Normal cell proliferation rate	$1.2\,\text{day}^{-1}$
b_1	Inverse of tumor cell carrying capacity	$1 \times 10^{-4}\,\text{cells}^{-1}\,\text{day}^{-1}$
b_2	Inverse of normal cell carrying capacity	$1\,\text{day}^{-1}$
η_1	Fraction of T-cell killing by normal cells without ligands	$1 \times 10^{-4}\,\text{cells}^{-1}\,\text{day}^{-1}$
η_2	Normal cell inactivation rate due to tumor cells	$5.553 \times 10^{-5}\,\text{cells}^{-1}\,\text{day}^{-1}$
d	Drug degradation rate	$1\,\text{day}^{-1}$

4. Existence and uniqueness

To facilitate the analysis and numerical implementation, the system of Eqs (3.1)–(3.5) can be expressed in a compact matrix-vector form. We define the state vector $\mathcal{Z}(\varsigma)$ to collect all state variables, while the interaction terms, including bilinear products such as $\mathbb{E}(\varsigma)\mathbb{I}(\varsigma)$ and $\mathbb{T}(\varsigma)\mathbb{N}(\varsigma)$, are systematically organized using constant matrices A_1, A_2, A_3, A_4. This formulation preserves the structure of the original system while enabling systematic theoretical analysis under the Hilfer fractional derivative.

Consider the system (3.1)–(3.5) with initial conditions

$$\mathbb{E}(\varsigma) \geq 0, \quad \mathbb{T}(\varsigma) \geq 0, \quad \mathbb{I}(\varsigma) \geq 0, \quad \mathbb{N}(\varsigma) \geq 0, \quad \mathbb{U}(\varsigma) \geq 0.$$

The system can be expressed as

$$\begin{cases} {}^{\mathcal{H}}\mathcal{D}_{0+}^{\alpha,\beta}\mathcal{Z}(\varsigma) = A_1\mathcal{Z}(\varsigma) + \mathbb{E}(\varsigma)A_2\mathcal{Z}(\varsigma) + \mathbb{T}(\varsigma)A_3\mathcal{Z}(\varsigma) + \mathbb{N}(\varsigma)A_4\mathcal{Z}(\varsigma) + A_5, \\ \mathcal{Z}(0) = \mathcal{Z}_0, \end{cases} \tag{4.1}$$

where

$$\mathcal{Z}(\varsigma) = \begin{pmatrix} \mathbb{E}(\varsigma) \\ \mathbb{T}(\varsigma) \\ \mathbb{I}(\varsigma) \\ \mathbb{N}(\varsigma) \\ \mathbb{U}(\varsigma) \end{pmatrix}, \quad \mathcal{Z}(0) = \begin{pmatrix} \mathbb{E}(0) \\ \mathbb{T}(0) \\ \mathbb{I}(0) \\ \mathbb{N}(0) \\ \mathbb{U}(0) \end{pmatrix}.$$

$$A_1 = \begin{pmatrix} -\mu_1^{\alpha,\beta} - \gamma_1^{\alpha,\beta}(1-e^{-U}) & \zeta^{\alpha,\beta} & 0 & 0 & 0 \\ 0 & a_1^{\alpha,\beta} - \gamma_2^{\alpha,\beta}(1-e^{-U}) & 0 & 0 & 0 \\ 0 & 0 & -\mu_2^{\alpha,\beta} & 0 & 0 \\ 0 & 0 & 0 & a_2^{\alpha,\beta} - \gamma_3^{\alpha,\beta}(1-e^{-U}) & 0 \\ 0 & 0 & 0 & 0 & -d^{\alpha,\beta} \end{pmatrix},$$

$$A_2 = \begin{pmatrix} 0 & 0 & g_1^{\alpha,\beta} & 0 & 0 \\ 0 & -g_2^{\alpha,\beta} & 0 & 0 & 0 \\ 0 & g_3^{\alpha,\beta} & 0 & 0 & 0 \\ 0 & 0 & 0 & 0 & 0 \\ 0 & 0 & 0 & 0 & 0 \end{pmatrix}, \quad A_3 = \begin{pmatrix} 0 & 0 & 0 & 0 & 0 \\ 0 & -a_1^{\alpha,\beta} b_1 & 0 & -\eta_1^{\alpha,\beta} & 0 \\ 0 & 0 & 0 & 0 & 0 \\ 0 & 0 & 0 & -\eta_2^{\alpha,\beta} & 0 \\ 0 & 0 & 0 & 0 & 0 \end{pmatrix},$$

$$A_4 = \begin{pmatrix} 0 & 0 & 0 & 0 & 0 \\ 0 & 0 & 0 & 0 & 0 \\ 0 & 0 & 0 & 0 & 0 \\ 0 & 0 & 0 & -a_2^{\alpha,\beta} b_2 & 0 \\ 0 & 0 & 0 & 0 & 0 \end{pmatrix}, \quad A_5 = \begin{pmatrix} w(\varsigma) s_1^{\alpha,\beta} \\ 0 \\ s_2^{\alpha,\beta} \\ 0 \\ v(\varsigma) \end{pmatrix}.$$

Definition 4.1. *Let $C^*[0,s]$ denote the class of continuous column vectors $\mathcal{Z}(\varsigma)$ whose components $\mathbb{E}(\varsigma)$, $\mathbb{T}(\varsigma)$, $\mathbb{I}(\varsigma)$, $\mathbb{N}(\varsigma)$, $\mathbb{U}(\varsigma)$ belong to $C^*[0,s]$, the space of continuous functions on the interval $[0,s]$. The norm of $\mathcal{Z} \in C^*[0,s]$ is defined by*

$$\|\mathcal{Z}\| = \sup_{\varsigma} |e^{-n\varsigma}\mathbb{E}(\varsigma)| + \sup_{\varsigma} |e^{-n\varsigma}\mathbb{T}(\varsigma)| + \sup_{\varsigma} |e^{-n\varsigma}\mathbb{I}(\varsigma)| + \sup_{\varsigma} |e^{-n\varsigma}\mathbb{N}(\varsigma)| + \sup_{\varsigma} |e^{-n\varsigma}\mathbb{U}(\varsigma)|,$$

where n is any natural number. When $\varsigma > \delta > m$, we denote $C^*_\delta[0,s]$ and $C_\delta[0,s]$ accordingly.

Definition 4.2. *A function $\mathcal{Z}$ is a solution of the system* (4.1) *if the following conditions hold:*

- $(\varsigma, \mathcal{Z}(\varsigma)) \in \Omega$, *where* $\varsigma \in [0,s]$, *and*

$$\Omega = [0,s] \times \Theta, \quad \Theta = \Big\{(\mathbb{E}(\varsigma), \mathbb{T}(\varsigma), \mathbb{I}(\varsigma), \mathbb{N}(\varsigma), \mathbb{U}(\varsigma)) \in \mathbb{R}^5_+ : |\mathbb{E}(\varsigma)| \le x,\ |\mathbb{T}(\varsigma)| \le y,\ |\mathbb{I}(\varsigma)| \le z,$$

$$|\mathbb{N}(\varsigma)| \le p,\ |\mathbb{U}(\varsigma)| \le q\Big\},$$

  where x, y, z, p, and q are positive constants.
- *The function $\mathcal{Z}(\varsigma)$ satisfies the system* (4.1).

Theorem 4.3. *The system* (4.1) *has a unique solution $\mathcal{Z} \in C^*[0,s]$.*

Proof. Applying the fractional integral operator $\mathcal{I}^{\alpha}_{0+}$ on both sides, we obtain

$$\mathcal{Z}(\varsigma) = \mathcal{Z}(0) + \mathcal{I}^{\alpha}_{0+}(A_1\mathcal{Z}(\varsigma) + \mathbb{E}(\varsigma)A_2\mathcal{Z}(\varsigma) + \mathbb{T}(\varsigma)A_3\mathcal{Z}(\varsigma) + \mathbb{N}(\varsigma)A_4\mathcal{Z}(\varsigma) + A_5). \tag{4.2}$$

Define the operator $\mathcal{T} : C^*[0,s] \to C^*[0,s]$ by

$$\mathcal{T}\mathcal{Z}(\varsigma) = \mathcal{Z}(0) + \mathcal{I}^{\alpha}_{0+}(A_1\mathcal{Z}(\varsigma) + \mathbb{E}(\varsigma)A_2\mathcal{Z}(\varsigma) + \mathbb{T}(\varsigma)A_3\mathcal{Z}(\varsigma) + \mathbb{N}(\varsigma)A_4\mathcal{Z}(\varsigma) + A_5). \tag{4.3}$$

Then,

$$\begin{aligned} e^{-n\varsigma}(\mathcal{T}\mathcal{Z}-\mathcal{T}\mathcal{Y}) &= e^{-n\varsigma}\mathcal{I}_{0+}^{\alpha}(A_1(\mathcal{Z}-\mathcal{Y})+\mathbb{E}(\varsigma)A_2(\mathcal{Z}-\mathcal{Y})+\mathbb{T}(\varsigma)A_3(\mathcal{Z}-\mathcal{Y})+\mathbb{N}(\varsigma)A_4(\mathcal{Z}-\mathcal{Y})) \\ &\leq \frac{1}{\Gamma(\alpha)}\int_0^{\varsigma}(\varsigma-s)^{\alpha-1}e^{-n(\varsigma-s)}e^{-ns}\|\mathcal{Z}-\mathcal{Y}\|(A_1+xA_2+yA_3+pA_4)ds \\ &= \frac{(A_1+xA_2+yA_3+pA_4)}{\Gamma(\alpha)}\|\mathcal{Z}-\mathcal{Y}\|\int_0^{\varsigma}(\varsigma-s)^{\alpha-1}e^{-n(\varsigma-s)}ds. \end{aligned}$$

Using the substitution $u = n(\varsigma - s)$, we get

$$\|\mathcal{T}\mathcal{Z}-\mathcal{T}\mathcal{Y}\| \leq \frac{(A_1+xA_2+yA_3+pA_4)}{n^{\alpha}}\|\mathcal{Z}-\mathcal{Y}\|.$$

If we choose n such that

$$n^{\alpha} > A_1 + xA_2 + yA_3 + pA_4,$$

then

$$\|\mathcal{T}\mathcal{Z}-\mathcal{T}\mathcal{Y}\| < \|\mathcal{Z}-\mathcal{Y}\|,$$

and by the Banach fixed-point theorem, the operator $\mathcal{T}$ has a unique fixed point. Thus, the system (4.1) has a unique solution $\mathcal{Z} \in C^*[0, s]$.

From Eq (4.2), we have

$$\begin{aligned} \mathcal{Z}(\varsigma) &= \mathcal{Z}(0)+\frac{\varsigma^{\alpha}}{\Gamma(\alpha+1)}(A_1\mathcal{Z}(0)+\mathbb{E}(0)A_2\mathcal{Z}(0)+\mathbb{T}(0)A_3\mathcal{Z}(0)+\mathbb{N}(0)A_4\mathcal{Z}(0)+A_5) \\ &\quad +\mathcal{I}_{0+}^{\alpha+1}(A_1\mathcal{Z}'(\varsigma)+\mathbb{E}(\varsigma)A_2\mathcal{Z}'(\varsigma)+\mathbb{E}'(\varsigma)A_2\mathcal{Z}(\varsigma)+\mathbb{T}'(\varsigma)A_3\mathcal{Z}(\varsigma)+\mathbb{T}(\varsigma)A_3\mathcal{Z}'(\varsigma) \\ &\quad +\mathbb{N}'(\varsigma)A_4\mathcal{Z}(\varsigma)+\mathbb{N}(\varsigma)A_4\mathcal{Z}'(\varsigma)). \end{aligned}$$

Differentiating with respect to ς, we obtain

$$\begin{aligned} \mathcal{Z}'(\varsigma) &= \frac{\varsigma^{\alpha-1}}{\Gamma(\alpha)}(A_1\mathcal{Z}(0)+\mathbb{E}(0)A_2\mathcal{Z}(0)+\mathbb{T}(0)A_3\mathcal{Z}(0)+\mathbb{N}(0)A_4\mathcal{Z}(0)+A_5) \\ &\quad +\mathcal{I}_{0+}^{\alpha}(A_1\mathcal{Z}'(\varsigma)+\mathbb{E}(\varsigma)A_2\mathcal{Z}'(\varsigma)+\mathbb{E}'(\varsigma)A_2\mathcal{Z}(\varsigma)+\mathbb{T}'(\varsigma)A_3\mathcal{Z}(\varsigma)+\mathbb{T}(\varsigma)A_3\mathcal{Z}'(\varsigma) \\ &\quad +\mathbb{N}'(\varsigma)A_4\mathcal{Z}(\varsigma)+\mathbb{N}(\varsigma)A_4\mathcal{Z}'(\varsigma)). \end{aligned}$$

Thus, $\mathcal{Z}' \in C_{\delta}^*[0, s]$. Applying $\mathcal{D}_{0+}^{\gamma}$ to *(7)*, we obtain

$${}^{\mathcal{H}}\mathcal{D}_{0+}^{\alpha,\beta}\mathcal{Z}(\varsigma) = A_1\mathcal{Z}(\varsigma)+\mathbb{E}(\varsigma)A_2\mathcal{Z}(\varsigma)+\mathbb{T}(\varsigma)A_3\mathcal{Z}(\varsigma)+\mathbb{N}(\varsigma)A_4\mathcal{Z}(\varsigma)+A_5.$$

Thus, the integral Eq (4.2) is equivalent to the system (4.1), completing the proof. □

Remark. The analytical method employed to establish the existence and uniqueness of the solution for the considered Hilfer fractional-order system is based on transforming the system into its equivalent Volterra-type integral form using fractional integral operators associated with the Hilfer derivative. This integral formulation enables the effective application of the Banach fixed-point theorem within a suitable Banach space of continuous functions. The use of this approach is particularly appropriate for Hilfer fractional-order models, as it rigorously handles the memory and nonlocal properties of

fractional derivatives while ensuring the mathematical well-posedness of the system under the assumed conditions. In this study, the order of the Hilfer fractional derivative is considered within the range $0.7 \leq \alpha \leq 1$, and the type parameter is taken in the range $0 \leq \beta \leq 1$. This selection effectively captures memory effects while maintaining system stability, biological relevance, and numerical convergence in the chemo-immunotherapy model. Lower values of α below 0.7 may introduce excessive memory effects and unrealistic slow decay in tumor dynamics, while the chosen range allows for an accurate balance between treatment efficacy and system stability under the proposed optimal control strategy. This result provides a foundational step for the subsequent analysis of the associated optimal control problem.

5. Stability analysis

Consider the fractional-order system:

$$\begin{cases} {}^{\mathcal{H}}\mathcal{D}_{0+}^{\alpha,\beta}\mathbb{E}(\varsigma) = 0, \\ {}^{\mathcal{H}}\mathcal{D}_{0+}^{\alpha,\beta}\mathbb{T}(\varsigma) = 0, \\ {}^{\mathcal{H}}\mathcal{D}_{0+}^{\alpha,\beta}\mathbb{I}(\varsigma) = 0, \\ {}^{\mathcal{H}}\mathcal{D}_{0+}^{\alpha,\beta}\mathbb{N}(\varsigma) = 0, \\ {}^{\mathcal{H}}\mathcal{D}_{0+}^{\alpha,\beta}\mathbb{U}(\varsigma) = 0. \end{cases}$$

That is,

$$\begin{cases} \zeta^{\alpha,\beta}\mathbb{T} - \mu_1^{\alpha,\beta}\mathbb{E} + g_1^{\alpha,\beta}\mathbb{E}\mathbb{I} + w(\varsigma)s_1^{\alpha,\beta} - \gamma_1^{\alpha,\beta}(1 - e^{-\mathbb{U}})\mathbb{E} = 0, \\ a_1^{\alpha,\beta}\mathbb{T}(1 - b_1\mathbb{T}) - g_2^{\alpha,\beta}\mathbb{E}\mathbb{T} - \eta_1^{\alpha,\beta}\mathbb{N}\mathbb{T} - \gamma_2^{\alpha,\beta}(1 - e^{-\mathbb{U}})\mathbb{T} = 0, \\ g_3^{\alpha,\beta}\mathbb{E}\mathbb{T} - \mu_2^{\alpha,\beta}\mathbb{I} + s_2^{\alpha,\beta} = 0, \\ a_2^{\alpha,\beta}\mathbb{N}(1 - b_2\mathbb{N}) - \eta_2^{\alpha,\beta}\mathbb{T}\mathbb{N} - \gamma_3^{\alpha,\beta}(1 - e^{-\mathbb{U}})\mathbb{N} = 0, \\ v(\varsigma) - d^{\alpha,\beta}\mathbb{U} = 0. \end{cases}$$

We analyze the stability under two cases:

Case i. Without chemotherapy drugs.

Set $\mathbb{U}(\varsigma) = 0$, $w(\varsigma) = 1$.

(1) Tumor-free steady state (normal cells persist, tumor cells are zero):

$$P_1 = [E^*, 0, I^*, N^*, 0] = \left[\frac{-s_1^{\alpha,\beta}\mu_1^{\alpha,\beta}}{\mu_1^{\alpha,\beta}\mu_2^{\alpha,\beta} + g_1^{\alpha,\beta}s_2^{\alpha,\beta}}, 0, \frac{s_2^{\alpha,\beta}}{\mu_2^{\alpha,\beta}}, \frac{1}{b_2}, 0\right].$$

(2) Tumor-present steady state:

$$P_2 = [E^*, T^*, I^*, N^*, 0] = \left[\frac{-(s_1^{\alpha,\beta} + \zeta^{\alpha,\beta}T^*)}{g_1^{\alpha,\beta} - \mu_1^{\alpha,\beta}}, \frac{a_1^{\alpha,\beta}}{a_1^{\alpha,\beta}b_1 + g_2^{\alpha,\beta} + \eta_1^{\alpha,\beta}}, \frac{g_3^{\alpha,\beta}E^*T^* + s_2^{\alpha,\beta}}{\mu_2^{\alpha,\beta}}, \frac{a_2^{\alpha,\beta} - \eta_2^{\alpha,\beta}T^*}{a_2^{\alpha,\beta}b_2}, 0\right].$$

Case ii. With chemotherapy drugs.

In this case, the drug component $\mathbb{U}(\varsigma)$ is active.

(3) The steady-state becomes:

$$P_3 = [E^*, T^*, I^*, N^*, U^*] = \left[\frac{\zeta^{\alpha,\beta}T^* + w(\varsigma)s_1^{\alpha,\beta}}{\mu_1^{\alpha,\beta} - g_1^{\alpha,\beta}T^* + \gamma_1^{\alpha,\beta}(1-e^{-U^*})}, \frac{a_1^{\alpha,\beta} - g_2^{\alpha,\beta}E^* - \eta_1^{\alpha,\beta}N^* - \gamma_2^{\alpha,\beta}(1-e^{-U^*})}{a_1^{\alpha,\beta}b_1},\right.$$
$$\left.\frac{g_3^{\alpha,\beta}E^*T^* + s_2^{\alpha,\beta}}{\mu_2^{\alpha,\beta}}, \frac{a_2^{\alpha,\beta} - \eta_2^{\alpha,\beta}T^* - \eta_1^{\alpha,\beta}N^* - \gamma_3^{\alpha,\beta}(1-e^{-U^*})}{a_2^{\alpha,\beta}b_2}, \frac{v(\varsigma)}{d^{\alpha,\beta}}\right].$$

These equilibrium points will be used in the subsequent linearization and eigenvalue-based stability analysis to determine local asymptotic stability under the Hilfer fractional operator framework.

Theorem 5.1. *Let P_1 be the equilibrium point of system (4.1). Then, P_1 is locally asymptotically stable.*

Proof. The Jacobian matrix of system (4.1) is

$$\mathcal{J}(P_1) = \begin{pmatrix} \Upsilon_1 & \zeta^{\alpha,\beta} & g_1^{\alpha,\beta}\mathbb{E}(\varsigma) & 0 & \gamma_1^{\alpha,\beta}e^{-\mathbb{U}(\varsigma)}\mathbb{E}(\varsigma) \\ g_2^{\alpha,\beta}\mathbb{T}(\varsigma) & \Upsilon_2 & 0 & -\eta_1^{\alpha,\beta}\mathbb{T}(\varsigma) & \gamma_2^{\alpha,\beta}e^{-\mathbb{U}(\varsigma)}\mathbb{T}(\varsigma) \\ g_3^{\alpha,\beta}\mathbb{T}(\varsigma) & g_3^{\alpha,\beta}\mathbb{E}(\varsigma) & -\mu_2^{\alpha,\beta} & 0 & 0 \\ 0 & -\eta_2^{\alpha,\beta}\mathbb{N}(\varsigma) & 0 & \Upsilon_3 & \gamma_3^{\alpha,\beta}e^{-\mathbb{U}(\varsigma)}\mathbb{N}(\varsigma) \\ 0 & 0 & 0 & 0 & -d^{\alpha,\beta} \end{pmatrix},$$

where

$$\Upsilon_1 = -\mu_1^{\alpha,\beta} + g_1^{\alpha,\beta}\mathbb{I}(\varsigma) - \gamma_1^{\alpha,\beta}(1-e^{-\mathbb{U}(\varsigma)}),$$
$$\Upsilon_2 = a_1^{\alpha,\beta} - a_1^{\alpha,\beta}b_1\mathbb{T}(\varsigma) - g_2^{\alpha,\beta}\mathbb{E}(\varsigma) - \eta_1^{\alpha,\beta}\mathbb{N}(\varsigma) - \gamma_2^{\alpha,\beta}(1-e^{-\mathbb{U}(\varsigma)}),$$
$$\Upsilon_3 = a_2^{\alpha,\beta} - a_2^{\alpha,\beta}b_2\mathbb{N}(\varsigma) - \eta_2^{\alpha,\beta}\mathbb{T}(\varsigma) - \gamma_3^{\alpha,\beta}(1-e^{-\mathbb{U}(\varsigma)}).$$

At P_1, the Jacobian simplifies to:

$$\mathcal{J}(P_1) = \begin{pmatrix} \left(\frac{-\mu_1\mu_2+g_1s_2}{\mu_2}\right)^{\alpha,\beta} & \zeta^{\alpha,\beta} & \left(\frac{-g_1s_1\mu_1}{\mu_1\mu_2+g_1s_2}\right)^{\alpha,\beta} & 0 & \left(\frac{\gamma_1s_1\mu_1}{\mu_1\mu_2+g_1s_2}\right)^{\alpha,\beta} \\ 0 & \left(a_1 + \frac{g_2s_1\mu_1}{\mu_1\mu_2+g_1s_2} - \frac{\eta_1}{b_2}\right)^{\alpha,\beta} & 0 & 0 & 0 \\ 0 & \left(\frac{-g_3s_1\mu_1}{\mu_1\mu_2+g_1s_2}\right)^{\alpha,\beta} & -\mu_2^{\alpha,\beta} & 0 & 0 \\ 0 & \left(\frac{-\eta_2}{b_2}\right)^{\alpha,\beta} & 0 & -a_2^{\alpha,\beta} & \left(\frac{\gamma_3}{b_2}\right)^{\alpha,\beta} \\ 0 & 0 & 0 & 0 & -d^{\alpha,\beta} \end{pmatrix}.$$

The eigenvalues of $\mathcal{J}(P_1)$ are:

$$\phi_1 = -\mu_2^{\alpha,\beta}, \quad \phi_2 = -d^{\alpha,\beta}, \quad \phi_3 = -\gamma_1^{\alpha,\beta},$$
$$\phi_4 = -\left(\frac{\mu_1\mu_2 - g_1s_2}{\mu_2}\right)^{\alpha,\beta}, \quad \phi_5 = \left(\frac{\eta_1 - a_1b_2}{b_2} + \frac{\mu_1g_2s_1}{\mu_1\mu_2 + g_1s_2}\right)^{\alpha,\beta}.$$

Since $\phi_i < 0$, we have $|\arg(\phi_i)| = \pi > \frac{\alpha\pi}{2}$ for $i = 1, 2, 3, 4$. If

$$\left(\frac{\eta_1}{b_2} + \frac{\mu_1 g_2 s_1}{\mu_1\mu_2 + g_1 s_2}\right)^{\alpha,\beta} < a_1^{\alpha,\beta},$$

then $\phi_5 < 0$, and $|\arg(\phi_5)| = \pi > \frac{\alpha\pi}{2}$.

Thus, by Theorem 2.5, the system at P_1 is locally asymptotically stable. □

Theorem 5.2. *Let P_2 be the equilibrium point of system (4.1). Then, P_2 is locally asymptotically stable.*

Proof. The Jacobian matrix of the model (4.1) is

$$\mathcal{J}(P_2) = \begin{pmatrix} \mathcal{G}_1 & \zeta^{\alpha,\beta} & \mathcal{G}_2 & 0 & \mathcal{G}_3 \\ \mathcal{G}_4 & \mathcal{G}_5 & 0 & \mathcal{G}_6 & \mathcal{G}_7 \\ \mathcal{G}_8 & \mathcal{G}_9 & -\mu_2^{\alpha,\beta} & 0 & 0 \\ 0 & \mathcal{G}_{10} & 0 & \mathcal{G}_{11} & \mathcal{G}_{12} \\ 0 & 0 & 0 & 0 & -d^{\alpha,\beta} \end{pmatrix},$$

where

$$\mathcal{G}_1 = \left(-\mu_1 + \frac{g_1 s_2}{\mu_2} - \frac{a_1 g_1 g_3}{\mu_2(g_1 - \mu_1)(a_1 b_1 + g_2 + \eta_2)}\left(s_1 - \frac{\zeta a_1}{a_1 b_1 + g_2 + \eta_2}\right) + \frac{g_1 s_2}{\mu_2}\right)^{\alpha,\beta},$$

$$\mathcal{G}_2 = \left(\frac{-g_1 s_1}{g_1 - \mu_1} - \frac{\zeta a_1 g_1}{(g_1 - \mu_1)(a_1 b_1 + g_2 + \eta_2)}\right)^{\alpha,\beta},$$

$$\mathcal{G}_3 = \left(\frac{-\gamma_1}{g_1 - \mu_1}\left(s_1 + \frac{\zeta a_1}{a_1 b_1 + g_2 + \eta_2}\right)\right)^{\alpha,\beta},$$

$$\mathcal{G}_4 = \left(\frac{-a_1 g_2}{a_1 b_1 + g_2 + \eta_2}\right)^{\alpha,\beta},$$

$$\mathcal{G}_5 = \left(a_1 - \frac{2a_1^2 b_1}{a_1 b_1 + g_2 + \eta_2} + \frac{g_2 s_1(a_1 b_1 + g_2 + \eta_2) + g_2 a_1 \zeta}{g_1 - \mu_1} - \frac{\eta_1}{b_2}(a_1 b_1 + g_2 + \eta_2) - \frac{\eta_1 \eta_2 a_1}{a_2 b_2}\right)^{\alpha,\beta},$$

$$\mathcal{G}_6 = \left(\frac{-\eta_1 a_1}{a_1 b_1 + g_2 + \eta_2}\right)^{\alpha,\beta}, \quad \mathcal{G}_7 = \left(\frac{a_1 \gamma_2}{a_1 b_1 + g_2 + \eta_2}\right)^{\alpha,\beta},$$

$$\mathcal{G}_8 = \left(\frac{a_1 g_3}{a_1 b_1 + g_2 + \eta_2}\right)^{\alpha,\beta},$$

$$\mathcal{G}_9 = \left(\frac{-g_3}{g_1 - \mu_1}(s_1(a_1 b_1 + g_2 + \eta_2) + \zeta_1)\right)^{\alpha,\beta},$$

$$\mathcal{G}_{10} = \left(\frac{\eta_2^2 a_1}{a_2 b_2} - \frac{\eta_2(a_1 b_1 + g_2 + \eta_2)}{b_2}\right)^{\alpha,\beta},$$

$$\mathcal{G}_{11} = \left(a_2 - 2a_2(a_1 b_1 + g_2 + \eta_2) + 2a_1\eta_2 - \frac{a_1 \eta_2}{a_1 b_1 + g_2 + \eta_2}\right)^{\alpha,\beta},$$

$$\mathcal{G}_{12} = \left(\frac{\gamma_3}{b_2}(a_1 b_1 + g_2 + \eta_2) - \frac{\gamma_3 \eta_2 a_1}{a_2 b_2}\right)^{\alpha,\beta}.$$

The characteristic equation is

$$(-d^{\alpha,\beta}-\phi)\Big(-\mathcal{G}_{10}\mathcal{G}_9(-\mathcal{G}_2\mathcal{G}_8+(\mathcal{G}_1-\phi)(-\phi+\mu))$$
$$+(\mathcal{G}_{11}-\phi)(-\mathcal{G}_4(\zeta(-\phi+\mu)-\mathcal{G}_2\mathcal{G}_9)+(\mathcal{G}_5-\phi)(-\mathcal{G}_2\mathcal{G}_8+(\mathcal{G}_1-\phi)(\phi+\mu)))\Big)=0.$$

We assume that all parameters are positive and all $\mathcal{G}_i$, $i=1,2,\ldots,12$, are positive. Using the Routh-Hurwitz criteria, we conclude that all eigenvalues are negative or have negative real parts. Hence, P_2 is locally asymptotically stable. □

Theorem 5.3. *Let P_3 be the equilibrium point of system (4.1). Then, P_3 is locally asymptotically stable.*

Proof. The Jacobian matrix of the model (4.1) evaluated at the equilibrium point P_3 is given by

$$\mathcal{J}(P_3)=\begin{pmatrix}\mathcal{F}_1 & \zeta^{\alpha,\beta} & \mathcal{F}_2 & 0 & \mathcal{F}_3\\ \mathcal{F}_4 & \mathcal{F}_5 & 0 & \mathcal{F}_6 & \mathcal{F}_7\\ \mathcal{F}_8 & \mathcal{F}_9 & -\mu_2^{\alpha,\beta} & 0 & 0\\ 0 & \mathcal{F}_{10} & 0 & \mathcal{F}_{11} & \mathcal{F}_{12}\\ 0 & 0 & 0 & 0 & -d^{\alpha,\beta}\end{pmatrix},$$

where

$$\mathcal{F}_1=\left(-\mu_1+\frac{g_1}{\mu_2}(g_3\mathbb{E}(\varsigma)\mathbb{T}(\varsigma)+s_2)-\gamma_1(1-e^{-\mathbb{U}(\varsigma)})\right)^{\alpha,\beta},$$
$$\mathcal{F}_2=\left(\frac{g_1(\zeta\mathbb{T}(\varsigma)+w(\varsigma)s_1)}{\mu_1-g_1\mathbb{T}(\varsigma)+\gamma_1(1-e^{\mathbb{U}(\varsigma)})}\right)^{\alpha,\beta},$$
$$\mathcal{F}_3=\left(\frac{\gamma_1e^{-\mathbb{U}(\varsigma)}(\zeta\mathbb{T}(\varsigma)+w(\varsigma)s_1)}{\mu_1-g_1\mathbb{T}(\varsigma)+\gamma_1(1-e^{\mathbb{U}(\varsigma)})}\right)^{\alpha,\beta},$$
$$\mathcal{F}_4=\left(\frac{-g_2}{a_1b_1}(a_1-g_2\mathbb{E}(\varsigma)-\eta_1\mathbb{N}(\varsigma)-\gamma_2(1-e^{-\mathbb{U}(\varsigma)})\right)^{\alpha,\beta},$$
$$\mathcal{F}_5=\left(a_1-2(a_1-g_2\mathbb{E}(\varsigma)-\eta_1\mathbb{N}(\varsigma)-\gamma_2(1-e^{-\mathbb{U}(\varsigma)})-g_2\frac{\zeta\mathbb{T}(\varsigma)+w(\varsigma)s_1)}{\mu_1-g_1\mathbb{T}(\varsigma)+\gamma_1(1-e^{\mathbb{U}(\varsigma)})}\right)^{\alpha,\beta},$$
$$\mathcal{F}_6=\left(\frac{-\eta_1}{a_1b_1}(a_1-g_2\mathbb{E}(\varsigma)-\eta_1\mathbb{N}(\varsigma)-\gamma_2(1-e^{-\mathbb{U}(\varsigma)})\right)^{\alpha,\beta},$$
$$\mathcal{F}_7=\left(\frac{\gamma_2e^{-\mathbb{U}(\varsigma)}}{a_1b_1}(a_1-g_2\mathbb{E}(\varsigma)-\eta_1\mathbb{N}(\varsigma)-\gamma_2(1-e^{-\mathbb{U}(\varsigma)})\right)^{\alpha,\beta},$$
$$\mathcal{F}_8=\left(\frac{g_3}{a_1b_1}(a_1-g_2\mathbb{E}(\varsigma)-\eta_1\mathbb{N}(\varsigma)-\gamma_2(1-e^{-\mathbb{U}(\varsigma)})\right)^{\alpha,\beta},$$
$$\mathcal{F}_9=\left(g_3\frac{(\zeta\mathbb{T}(\varsigma)+w(\varsigma)s_1)}{\mu_1-g_1\mathbb{T}(\varsigma)+\gamma_1(1-e^{\mathbb{U}(\varsigma)})}\right)^{\alpha,\beta},$$
$$\mathcal{F}_{10}=\left(\frac{-\eta_2}{a_2b_2}(a_2-(\eta_1+\eta_2)\mathbb{T}(\varsigma)-\gamma_3(1-e^{-\mathbb{U}(\varsigma)})\right)^{\alpha,\beta},$$
$$\mathcal{F}_{11}=\left(-a_2-(\eta_1\eta_2)\mathbb{T}(\varsigma)-\gamma_3(1-e^{-\mathbb{U}(\varsigma)})\frac{-\eta_2}{a_1b_1}(a_1-g_2\mathbb{E}(\varsigma)-\eta_1\mathbb{N}(\varsigma)-\gamma_2(1-e^{-\mathbb{U}(\varsigma)})-\gamma_3(1-e^{-\mathbb{U}(\varsigma)})\right)^{\alpha,\beta},$$

$$\mathcal{F}_{12} = \left(\frac{\gamma_3 e^{-\mathbb{U}(\varsigma)}}{a_2 b_2}(a_2 - (\eta_1 + \eta_2)\mathbb{T}(\varsigma) - \gamma_3(1 - e^{-\mathbb{U}(\varsigma)})\right)^{\alpha,\beta}.$$

The characteristic equation of the Jacobian at P_3 is

$$\left\{\begin{array}{c} \phi^4 + \phi^3(\mathcal{F}_6\mathcal{F}_{10} - \mathcal{F}_{11} - \mathcal{F}_5 - \mathcal{F}_1 + \mu_2) + \phi^2(d\mathcal{F}_6\mathcal{F}_{10} - \mathcal{F}_6\mathcal{F}_{10}\mathcal{F}_6\mathcal{F}_1 + \mu\mathcal{F}_6\mathcal{F}_{10} + \mathcal{F}_5\mathcal{F}_{11} + \mathcal{F}_1\mathcal{F}_{11} - \mathcal{F}_{11}\mu \\ -\mathcal{F}_8\mathcal{F}_2 + \mathcal{F}_5\mathcal{F}_1 - \mathcal{F}_5\mu_2 - \mathcal{F}_1\mu_2) + \phi(-d\mathcal{F}_6\mathcal{F}_{10}\mathcal{F}_1 + d\mu_2\mathcal{F}_6\mathcal{F}_{10} - \mathcal{F}_6\mathcal{F}_{10}\mathcal{F}_8\mathcal{F}_2 - \mu_2\mathcal{F}_6\mathcal{F}_{10}\mathcal{F}_1 + \mathcal{F}_{11}\mathcal{F}_8\mathcal{F}_2 \\ -\mathcal{F}_{11}\mathcal{F}_5\mathcal{F}_1 + \mu_2\mathcal{F}_{11}\mathcal{F}_5 + \mu_2\mathcal{F}_{11}\mathcal{F}_1 + \mathcal{F}_8\mathcal{F}_2\mathcal{F}_5 + \mu_2\mathcal{F}_5\mathcal{F}_1 + \zeta\mathcal{F}_4) + d\mathcal{F}_{10}\mathcal{F}_6\mathcal{F}_8\mathcal{F}_2 - d\mu_2\mathcal{F}_1\mathcal{F}_{10} + \mu_2\mathcal{F}_1\mathcal{F}_5\mathcal{F}_{11} \\ -\mu_2\mathcal{F}_1\mathcal{F}_5\mathcal{F}_{11} + \zeta\mu_2\mathcal{F}_4 + \mathcal{F}_2\mathcal{F}_4\mathcal{F}_9 \end{array}\right\} = 0.$$

Assuming that all parameters are positive and all $\mathcal{F}_i > 0$, it follows that all $a_i > 0$. By the Routh-Hurwitz criteria, all eigenvalues of the Jacobian matrix will have negative real parts.

Hence, the equilibrium point P_3 is locally asymptotically stable. □

6. Optimal control analysis

Consider the state system (3.1)–(3.5) in $\mathbb{R}^5$. Let

$$\Omega = \left\{(v(\varsigma), w(\varsigma)) \text{ are Lebesgue measurable} : 0 \le v(\varsigma) \le v_{\max} < \infty,\ 0 \le w(\varsigma) \le w_{\max} < \infty,\ \forall \varsigma \in [0, \varsigma_f]\right\}$$

be the admissible control set, where ς_f is the final time.

The objective functional is given by

$$J(v(\varsigma), w(\varsigma)) = \int_0^{\varsigma_f} \left[\mathbb{E}(\varsigma) + \mathbb{I}(\varsigma) - \mathbb{T}(\varsigma) - \frac{1}{2}\left(Av^2(\varsigma) + Bw^2(\varsigma)\right)\right] d\varsigma,$$

where the weight factors A and B represent the tolerability of chemotherapy and external immunotherapy by the patient.

The aim is to maximize the functional

$$J(v(\varsigma), w(\varsigma)) = \int_0^{\varsigma_f} L(\mathbb{E}(\varsigma), \mathbb{T}(\varsigma), \mathbb{I}(\varsigma), \mathbb{N}(\varsigma), \mathbb{U}(\varsigma), v(\varsigma), w(\varsigma), \varsigma) d\varsigma,$$

subject to the constraints

$$\begin{array}{ll} {}^{\mathcal{H}}\mathcal{D}_{0+}^{\alpha,\beta}\mathbb{E}(\varsigma) = \chi_1(\varsigma), & {}^{\mathcal{H}}\mathcal{D}_{0+}^{\alpha,\beta}\mathbb{T}(\varsigma) = \chi_2(\varsigma), \\ {}^{\mathcal{H}}\mathcal{D}_{0+}^{\alpha,\beta}\mathbb{I}(\varsigma) = \chi_3(\varsigma), & {}^{\mathcal{H}}\mathcal{D}_{0+}^{\alpha,\beta}\mathbb{N}(\varsigma) = \chi_4(\varsigma), \\ {}^{\mathcal{H}}\mathcal{D}_{0+}^{\alpha,\beta}\mathbb{U}(\varsigma) = \chi_5(\varsigma), & \end{array}$$

where

$$\chi_n(\varsigma) = \chi(\mathbb{E}(\varsigma), \mathbb{T}(\varsigma), \mathbb{I}(\varsigma), \mathbb{N}(\varsigma), \mathbb{U}(\varsigma), v(\varsigma), w(\varsigma), \varsigma), \quad n = 1, 2, \ldots, 5.$$

The initial conditions are

$$\mathbb{E}(0) \ge 0, \quad \mathbb{T}(0) \ge 0, \quad \mathbb{I}(0) \ge 0, \quad \mathbb{N}(0) \ge 0, \quad \mathbb{U}(0) \ge 0.$$

The Hamiltonian is defined as

$$H(\chi_n(\varsigma), \lambda(\varsigma), v(\varsigma), w(\varsigma)) = \mathbb{E}(\varsigma) - \mathbb{T}(\varsigma) + \mathbb{I}(\varsigma) - \frac{1}{2}\left(Av^2(\varsigma) + Bw^2(\varsigma)\right)$$

$$
\begin{aligned}
&+\lambda_1(\varsigma)\left({}^{\mathcal{H}}\mathcal{D}_{0+}^{\alpha,\beta}\mathbb{E}(\varsigma)\right)+\lambda_2(\varsigma)\left({}^{\mathcal{H}}\mathcal{D}_{0+}^{\alpha,\beta}\mathbb{T}(\varsigma)\right)\\
&+\lambda_3(\varsigma)\left({}^{\mathcal{H}}\mathcal{D}_{0+}^{\alpha,\beta}\mathbb{I}(\varsigma)\right)+\lambda_4(\varsigma)\left({}^{\mathcal{H}}\mathcal{D}_{0+}^{\alpha,\beta}\mathbb{N}(\varsigma)\right)\\
&+\lambda_5(\varsigma)\left({}^{\mathcal{H}}\mathcal{D}_{0+}^{\alpha,\beta}\mathbb{U}(\varsigma)\right).
\end{aligned}
$$

This leads to the following modified objective functional:

$$
J(v(\varsigma),w(\varsigma)) \;=\; \int_0^{\varsigma_f} H(\chi_{\mathbb{N}}(\varsigma),\lambda(\varsigma),v(\varsigma),w(\varsigma))-\sum_{i=1}^{5}\lambda_{\mathbb{I}}(\varsigma)^{\mathcal{H}}\mathcal{D}_{0+}^{\alpha,\beta}f(\chi_{\mathbb{N}}(\varsigma),v(\varsigma),w(\varsigma))dt.
$$

From the above, the necessary conditions for the fractional-order optimal control in the sense of Hilfer derivatives are

$$
\begin{aligned}
&{}^{\mathcal{H}}\mathcal{D}_{0+}^{\alpha,\beta}\lambda_1(\varsigma)=\left(\frac{\partial H(\varsigma)}{\partial\mathbb{E}(\varsigma)}\right), \quad {}^{\mathcal{H}}\mathcal{D}_{0+}^{\alpha,\beta}\lambda_2(\varsigma)=\left(\frac{\partial H(\varsigma)}{\partial\mathbb{T}(\varsigma)}\right),\\
&{}^{\mathcal{H}}\mathcal{D}_{0+}^{\alpha,\beta}\lambda_3(\varsigma)=\left(\frac{\partial H(\varsigma)}{\partial\mathbb{I}(\varsigma)}\right), \quad {}^{\mathcal{H}}\mathcal{D}_{0+}^{\alpha,\beta}\lambda_4(\varsigma)=\left(\frac{\partial H(\varsigma)}{\partial\mathbb{N}(\varsigma)}\right),\\
&{}^{\mathcal{H}}\mathcal{D}_{0+}^{\alpha,\beta}\lambda_5(\varsigma)=\left(\frac{\partial H(\varsigma)}{\partial\mathbb{U}(\varsigma)}\right).
\end{aligned}
$$

6.1. Boundedness and existence of an optimal control

Theorem 6.1. *An optimal control pair* $(v^*(\varsigma),w^*(\varsigma))\in\Omega$ *exists for the optimal control problem, such that*

$$
J(v(\varsigma),w(\varsigma))=J^*(v(\varsigma),w(\varsigma))=\max_{v(\varsigma),w(\varsigma)\in\Omega}J(v(\varsigma),w(\varsigma)),
$$

provided that the following conditions hold:

1. *The admissible control set is nonempty.*
2. *The set* Ω *of admissible controls is closed, convex, and nonempty.*
3. *The righthand side of the state system is bounded by a linear combination of the state and control variables.*
4. *The integrand of the objective functional is concave with respect to* Ω.
5. *There exist constants* $l_2,l_3>0$ *such that*

$$
L(\chi_{\mathbb{N}}(\varsigma),\lambda(\varsigma),v(\varsigma),w(\varsigma))\le l_2-l_3\left(|v(\varsigma)|+|w(\varsigma)|\right)^2.
$$

Proof. To verify the conditions above, we first prove the existence of a solution for system (3.1)–(3.5). Since

$$
g_1^{\alpha,\beta}\mathbb{I}(\varsigma)<g_1^{\alpha,\beta}, \quad v_{\max}<\infty,
$$

and by disregarding the negative terms in the model, we obtain the following inequalities:

$$
\begin{aligned}
&{}^{\mathcal{H}}\mathcal{D}_{0+}^{\alpha,\beta}\mathbb{E}(\varsigma)<s_1^{\alpha,\beta}+g_1^{\alpha,\beta}\mathbb{E}(\varsigma),\\
&{}^{\mathcal{H}}\mathcal{D}_{0+}^{\alpha,\beta}\mathbb{T}(\varsigma)<a_1^{\alpha,\beta}\mathbb{T}(\varsigma),\\
&{}^{\mathcal{H}}\mathcal{D}_{0+}^{\alpha,\beta}T_0(\varsigma)<s_2^{\alpha,\beta}+g_3^{\alpha,\beta}\mathbb{E}(\varsigma),
\end{aligned}
$$

$$
\begin{aligned}
{}^{\mathcal{H}}\mathcal{D}_{0+}^{\alpha,\beta}\mathbb{N}(\varsigma) &< a_1^{\alpha,\beta}\mathbb{N}(\varsigma),\\
{}^{\mathcal{H}}\mathcal{D}_{0+}^{\alpha,\beta}\mathbb{U}(\varsigma) &< v_{\max}.
\end{aligned}
$$

This system can be rewritten in vector form as:

$$
{}^{\mathcal{H}}\mathcal{D}_{0+}^{\alpha,\beta}\begin{pmatrix}\mathbb{E}(\varsigma)\\ \mathbb{T}(\varsigma)\\ \mathbb{I}(\varsigma)\\ \mathbb{N}(\varsigma)\\ \mathbb{U}(\varsigma)\end{pmatrix} = \begin{pmatrix} 0 & 0 & 0 & 0 & 0\\ 0 & a_1^{\alpha,\beta} & 0 & 0 & 0\\ g_3^{\alpha,\beta} & 0 & 0 & 0 & 0\\ 0 & 0 & 0 & a_2^{\alpha,\beta} & 0\\ 0 & 0 & 0 & 0 & 0\end{pmatrix}\begin{pmatrix}\mathbb{E}(\varsigma)\\ \mathbb{T}(\varsigma)\\ \mathbb{I}(\varsigma)\\ \mathbb{N}(\varsigma)\\ \mathbb{U}(\varsigma)\end{pmatrix} + \begin{pmatrix} s_1^{\alpha,\beta}\\ 0\\ s_2^{\alpha,\beta}\\ 0\\ v_{\max}\end{pmatrix}.
$$

This system has bounded coefficients and is linear within a finite time interval. Therefore, the solutions to this linear system are uniformly bounded. As a result, the solutions to the nonlinear system (3.1)–(3.5) are also bounded and exist, confirming that the first condition is satisfied.

The definition of Ω satisfies the second condition. System (3.1)–(3.5) is bilinear in the control variables $v(\varsigma)$ and $w(\varsigma)$, and can be expressed as

$$
f(\chi_{\mathbb{N}}(\varsigma), v(\varsigma), w(\varsigma)) = \psi(\varsigma, \chi_{\mathbb{N}}(\varsigma)) + s_1^{\alpha,\beta} + s_2^{\alpha,\beta} + v(\varsigma) + w(\varsigma),
$$

where ψ is a vector-valued function of $\chi_{\mathbb{N}}(\varsigma)$. Since the solutions are bounded, we have

$$
\begin{aligned}
|f(\chi_{\mathbb{N}}(\varsigma), v(\varsigma), w(\varsigma))| &\le |p_1\chi_{\mathbb{N}}(\varsigma)| + |p_2| + |p_3| + |p_4|\\
&\le n_1|\chi_{\mathbb{N}}(\varsigma)| + |s_1^{\alpha,\beta}| + |s_2^{\alpha,\beta}| + |v(\varsigma)| + |w(\varsigma)|,
\end{aligned}
$$

where n_1 depends on the system coefficients.

Additionally, we define the following matrices:

$$
p_1 = \begin{pmatrix} 0 & 0 & 0 & 0 & 0\\ 0 & a_1^{\alpha,\beta} & 0 & 0 & 0\\ g_3^{\alpha,\beta} & 0 & 0 & 0 & 0\\ 0 & 0 & 0 & a_2^{\alpha,\beta} & 0\\ 0 & 0 & 0 & 0 & 0\end{pmatrix}, \quad p_2 = \begin{pmatrix} s_1^{\alpha,\beta}\\ 0\\ 0\\ 0\\ 0\end{pmatrix}, \quad p_3 = \begin{pmatrix} 0\\ 0\\ s_2^{\alpha,\beta}\\ 0\\ 0\end{pmatrix}, \quad p_4 = \begin{pmatrix} 0\\ 0\\ 0\\ 0\\ v_{\max}\end{pmatrix}.
$$

It can also be observed that the integrand of the system's objective functional, $J(v(\varsigma), w(\varsigma))$, is concave. Specifically, we have

$$
\begin{aligned}
\mathbb{E}(\varsigma) + \mathbb{I}(\varsigma) - \mathbb{T}(\varsigma) - \tfrac{1}{2}(Av^2(\varsigma) + Bw^2(\varsigma)) &< \mathbb{E}(\varsigma) + \mathbb{I}(\varsigma) - \tfrac{1}{2}(Av^2(\varsigma) + Bw^2(\varsigma))\\
&\le n_2 - n_3(|v(\varsigma)|^2 + |w(\varsigma)|^2),
\end{aligned}
$$

where the upper bounds of $\mathbb{E}(\varsigma) + \mathbb{I}(\varsigma)$ define n_2, and $n_3 = \frac{A+B}{2}$.

Thus, the proof is complete, and we conclude that $v(\varsigma)$ and $w(\varsigma)$ are the optimal control variables.

6.2. Necessary conditions for fractional order optimal control

Theorem 6.2. *Let $v^*(\varsigma)$ and $w^*(\varsigma)$ be the optimal control variables, with corresponding state variables $E^*(\varsigma)$, $T^*(\varsigma)$, $I^*(\varsigma)$, $N^*(\varsigma)$, and $U^*(\varsigma)$. Then, there exist adjoint variables $\lambda_i^*(\varsigma)$ for $i = 1, 2, \ldots, 5$ that satisfy the following conditions:*

1. Adjoint equation: The adjoint variables must satisfy the following system of equations:

$$\begin{aligned}
{}^{\mathcal{H}}\mathcal{D}_{0+}^{\alpha,\beta}\lambda_1(\varsigma) &= 1+\lambda_1(\varsigma)\left(-\mu_1^{\alpha,\beta}+g_1^{\alpha,\beta}\mathbb{I}(\varsigma)-\gamma_1^{\alpha,\beta}(1-e^{-\mathbb{U}(\varsigma)})\right),\\
{}^{\mathcal{H}}\mathcal{D}_{0+}^{\alpha,\beta}\lambda_2(\varsigma) &= -1+\lambda_1(\varsigma)\zeta^{\alpha,\beta}+\lambda_2(\varsigma)\left(a_1^{\alpha,\beta}-2a_1^{\alpha,\beta}b_1\mathbb{T}(\varsigma)-g_2^{\alpha,\beta}\mathbb{E}(\varsigma)-\eta_1^{\alpha,\beta}\mathbb{N}(\varsigma)\right.\\
&\quad \left.-\gamma_2^{\alpha,\beta}(1-e^{-\mathbb{U}(\varsigma)})\right)+\lambda_3(\varsigma)\left(g_3^{\alpha,\beta}\mathbb{E}(\varsigma)\right)-\lambda_4(\varsigma)\left(\eta_2^{\alpha,\beta}\mathbb{N}(\varsigma)\right),\\
{}^{\mathcal{H}}\mathcal{D}_{0+}^{\alpha,\beta}\lambda_3(\varsigma) &= \lambda_1(\varsigma)\left(g_1^{\alpha,\beta}\mathbb{E}(\varsigma)\right)-\mu_2^{\alpha,\beta}\lambda_3(\varsigma),\\
{}^{\mathcal{H}}\mathcal{D}_{0+}^{\alpha,\beta}\lambda_4(\varsigma) &= -\lambda_2(\varsigma)\left(\eta_1^{\alpha,\beta}\mathbb{T}(\varsigma)\right)+\lambda_4(\varsigma)\left(a_2^{\alpha,\beta}-2a_2^{\alpha,\beta}b_2-\eta_2\mathbb{T}(\varsigma)-\gamma_3^{\alpha,\beta}(1-e^{-\mathbb{U}(\varsigma)})\right),\\
{}^{\mathcal{H}}\mathcal{D}_{0+}^{\alpha,\beta}\lambda_5(\varsigma) &= -\lambda_1(\varsigma)\left(\gamma_1^{\alpha,\beta}e^{-\mathbb{U}(\varsigma)}\right)-\lambda_2(\varsigma)\left(\gamma_2^{\alpha,\beta}e^{-\mathbb{U}(\varsigma)}\right)\\
&\quad -\lambda_4(\varsigma)\left(\gamma_3^{\alpha,\beta}e^{-\mathbb{U}(\varsigma)}\right)-d^{\alpha,\beta}\lambda_5(\varsigma).
\end{aligned}$$

2. Transversality condition: The adjoint variables must satisfy the following boundary conditions:

$$\lambda_i^*(\varsigma) = 0, \quad i=1,2,\ldots,5.$$

3. Optimality condition: The Hamiltonian must satisfy the following optimality condition:

$$\begin{aligned}
&H(\chi_{\mathbb{N}}(\varsigma),\lambda(\varsigma),v(\varsigma),w(\varsigma))\\
&=\max_{v(\varsigma),w(\varsigma)\in\Omega}\left\{H(\chi_{\mathbb{N}}(\varsigma),\lambda(\varsigma),v(\varsigma),w(\varsigma))\;\middle|\;0\le v(\varsigma)\le v_{max},\ 0\le w(\varsigma)\le w_{max}\right\}.
\end{aligned}$$

Furthermore, the optimal control variables are given by:

$$\begin{aligned}
v(\varsigma) &= \min\left\{\max\left\{0,\frac{\lambda_5(\varsigma)}{A}\right\},v_{max}\right\},\\
w(\varsigma) &= \min\left\{\max\left\{0,\frac{\lambda_1(\varsigma)s_1^{\alpha,\beta}}{B}\right\},w_{max}\right\}.
\end{aligned}$$

6.3. Numerical analysis for fractional order optimal control

In this section, we present a numerical analysis using MATLAB to solve the optimality system (3.1)–(3.5) under the transversality conditions

$$\lambda_i(\varsigma_f)=0, \quad i=1,\ldots,5,$$

where $\varsigma_f = 100$ is the final simulation time. The initial conditions for the state variables are set as follows:

$$\mathbb{E}(0)=1000, \quad \mathbb{T}(0)=400, \quad \mathbb{I}(0)=100, \quad \mathbb{N}(0)=0.9, \quad \mathbb{U}(0)=0.$$

The parameters used in these simulations are adopted from Table 2, and the fractional order α is taken within the range $0<\alpha\le 1$.

Figure 1 presents the numerical simulation of effector cell population dynamics over time in the absence of control interventions for different values of the fractional order α. Initially, the immune system responds to tumor growth by increasing the effector cell count, demonstrating its capability to recognize and target tumor cells. However, due to the rapid proliferation of tumor cells and the absence

of apoptotic mechanisms, the immune response alone becomes insufficient to control and eradicate the tumor effectively. This behavior highlights the critical need for incorporating optimal control strategies, such as chemotherapy and immunotherapy, to enhance the immune system's effectiveness in tumor clearance, particularly under fractional-order dynamics that reflect memory and hereditary properties of biological systems.

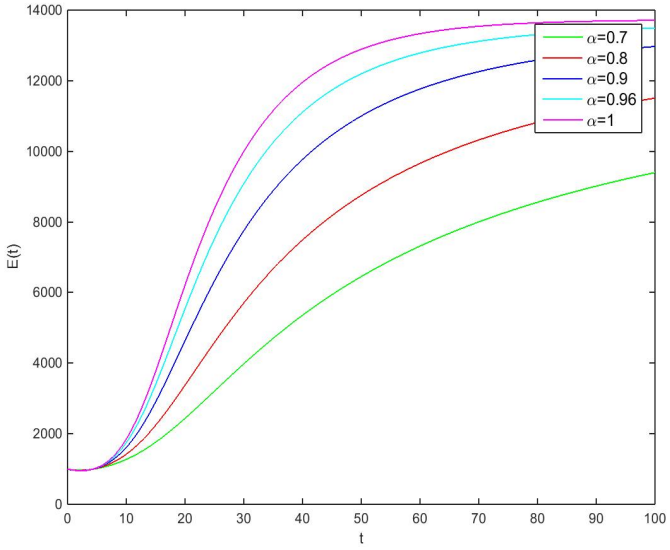

Figure 1. Effector cell dynamics without chemotherapy and immunotherapy under varying fractional orders $\alpha = 0.7, 0.8, 0.9, 0.96, 1$ and $\beta = 0.5$. The simulation illustrates the immune system's natural response to tumor growth without external intervention.

Both chemotherapy and immunotherapy contribute to the proliferation of effector cells, as depicted in Figure 2. In the absence of immunotherapy (Figure 2(a)), chemotherapy initially allows the effector cell population to increase; however, due to its cytotoxic effects, the effector cells decline over time. In contrast, the absence of chemotherapy (Figure 2(b)) while administering immunotherapy leads to the stimulation of effector cells, but the continued growth of the tumor eventually suppresses the immune response, causing the effector cell population to decrease gradually. These observations highlight the limitations of using either therapy in isolation and emphasize the significance of an optimal combined control strategy to sustain effector cell activity against tumor cells within a fractional-order framework.

Figure 3 presents the numerical simulations of effector cells under the simultaneous application of chemotherapy and immunotherapy within a fractional-order control framework. This combined approach demonstrates a synergistic effect in managing effector cell dynamics. Immunotherapy supports effector cell proliferation to enhance immune surveillance, while chemotherapy reduces the tumor burden, indirectly aiding the immune system. However, the immunosuppressive nature of chemotherapy also contributes to a gradual reduction in effector cells, maintaining a balanced immune response. The results indicate that combined therapeutic strategies under optimal fractional-order control can effectively manage tumor progression while sustaining an adequate immune response without leading to excessive effector cell proliferation.

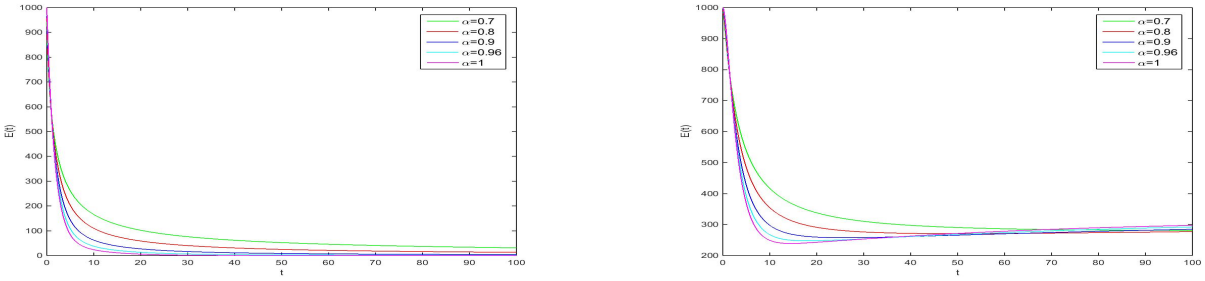

(a) Effector cells without immunotherapy **(b)** Effector cells without chemotherapy

Figure 2. Dynamics of effector cells under fractional-order dynamics ($\alpha = 0.7, 0.8, 0.9, 0.96, 1$ and $\beta = 0.5$) : (a) Without immunotherapy and (b) without chemotherapy. The figures illustrate the changes in effector cell populations under each scenario, demonstrating the need for combined therapeutic strategies for effective tumor control.

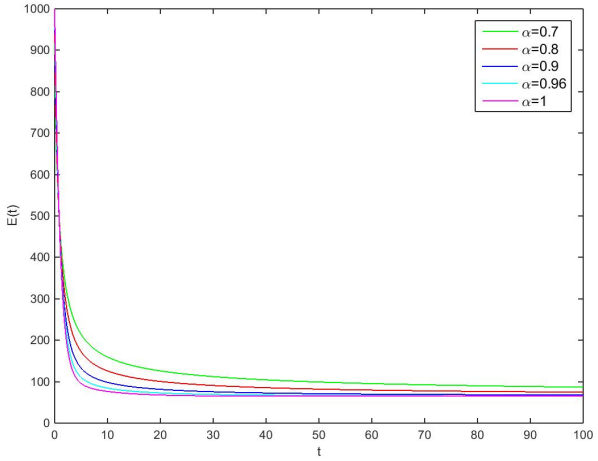

Figure 3. Effector cell dynamics under combined chemotherapy and immunotherapy for fractional orders $\alpha = 0.7, 0.8, 0.9, 0.96, 1$ and $\beta = 0.5$. The figure illustrates the balanced control of effector cell populations under the synergistic effects of both treatments, supporting effective anti-tumor activity while preventing excessive immune proliferation.

Figure 4 presents the numerical simulation of tumor cell dynamics over time in the absence of control interventions for different values of the fractional order α. The results demonstrate a steady and unchecked increase in the tumor cell population due to the lack of apoptosis or immune-mediated tumor clearance in the system. As the fractional order varies, the system captures the effects of memory and hereditary properties in biological processes, which influence the tumor growth rate. These results highlight the need for incorporating optimal control strategies, such as chemotherapy and immunotherapy, to effectively limit tumor proliferation, particularly within fractional-order models of tumor-immune dynamics.

The numerical simulations in Figure 5 illustrate the tumor cell dynamics under single-control strategies across different fractional orders α. In Figure 5(a), chemotherapy alone is applied, effectively slowing the proliferation of tumor cells by directly inhibiting their growth. In Figure 5(b),

immunotherapy alone is applied, enhancing immune-mediated tumor suppression and thereby reducing tumor cell numbers over time. Both strategies demonstrate a significant reduction in tumor cells compared to the uncontrolled scenario; however, neither approach alone fully eradicates the tumor population. These findings highlight the necessity of employing combined chemo-immunotherapy strategies under fractional-order modeling to achieve effective tumor control while accurately capturing the memory and hereditary properties inherent in biological systems.

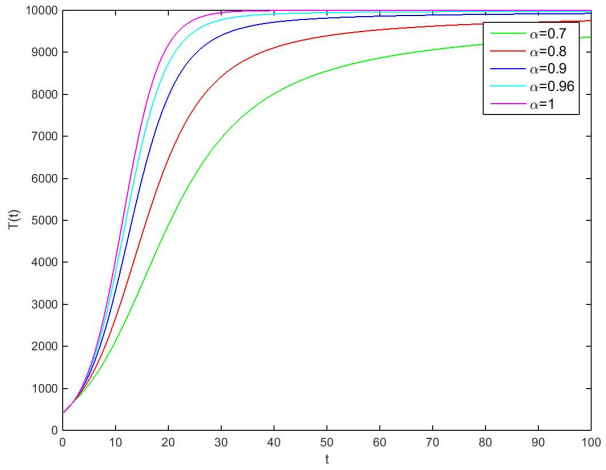

Figure 4. Tumor cell dynamics without chemotherapy and immunotherapy under varying fractional orders $\alpha = 0.7, 0.8, 0.9, 0.96, 1$ and $\beta = 0.5$. The simulation shows tumor proliferation in the absence of control interventions.

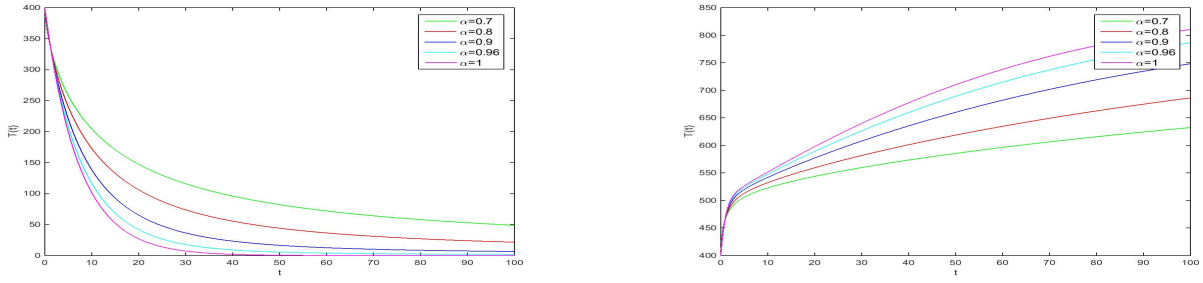

(a) Without immunotherapy (chemotherapy applied) **(b)** Without chemotherapy (immunotherapy applied)

Figure 5. Tumor cell dynamics under single-control strategies at fractional orders $\alpha = 0.7, 0.8, 0.9, 0.96, 1$ and $\beta = 0.5$. Each approach reduces tumor growth compared to the uncontrolled scenario, demonstrating the partial effectiveness of single-control methods under fractional-order dynamics.

Figure 6 presents the numerical simulations of tumor cell populations under the concurrent application of chemotherapy and immunotherapy across different fractional orders α. This combined control strategy significantly enhances tumor cell reduction compared to applying either therapy individually. The synergy between chemotherapy and immunotherapy under fractional-order dynamics, which capture the memory and hereditary characteristics of biological systems, contributes

to a more effective reduction in tumor cell numbers, highlighting the importance of integrated therapeutic approaches in cancer treatment.

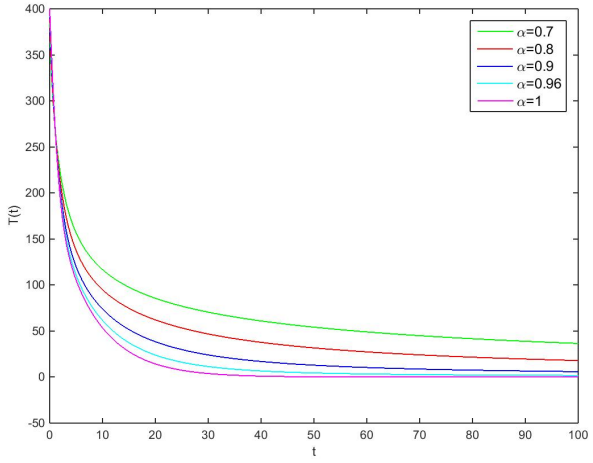

Figure 6. Tumor cell dynamics with combined chemotherapy and immunotherapy at fractional orders $\alpha = 0.7, 0.8, 0.9, 0.96, 1$ and $\beta = 0.5$. The combined treatment strategy significantly reduces tumor cell numbers compared to single-control or uncontrolled scenarios.

Figure 7 illustrates the numerical simulations of normal cell dynamics without the application of chemo-immunotherapy under various fractional orders α. In the absence of control measures, normal cell populations exhibit a gradual decline over time, reflecting the detrimental effects of unchecked tumor progression on healthy cells within the system. This trend emphasizes the need for effective control strategies to preserve normal cell populations while combating tumor growth in cancer therapy models governed by fractional-order dynamics.

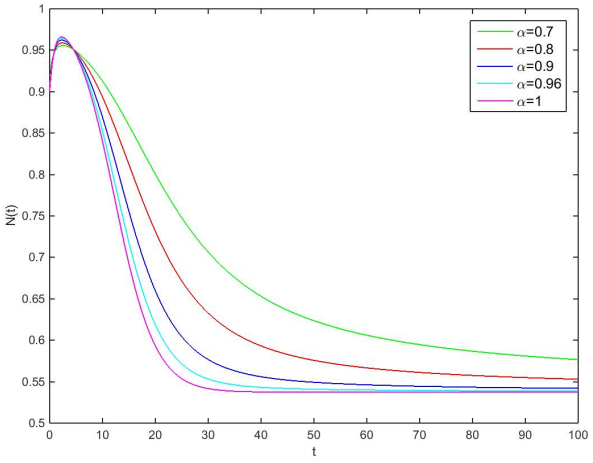

Figure 7. Normal cell dynamics without any controls at fractional orders $\alpha = 0.7, 0.8, 0.9, 0.96, 1$ and $\beta = 0.5$. Normal cell populations gradually diminish in the absence of chemo-immunotherapy.

Figure 8 presents the numerical simulations of normal cell populations under single-control strategies across different fractional orders α. In Figure 8(a), chemotherapy alone is applied, resulting in the gradual proliferation of normal cells by controlling the tumor's effect on healthy cells. In Figure 8(b), immunotherapy alone is administered, enhancing immune-mediated protection of normal cells and contributing to their steady increase over time. Both strategies promote the growth of healthy cells under fractional-order dynamics, highlighting the potential benefits of control strategies in preserving normal cell populations during cancer treatment.

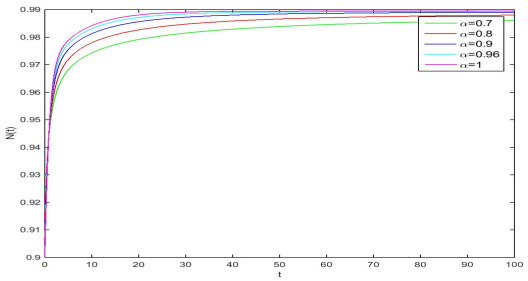

(a) Normal cells without immunotherapy (chemotherapy applied)

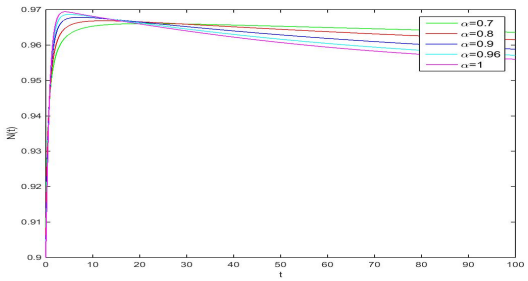

(b) Normal cells without chemotherapy (immunotherapy applied)

Figure 8. Normal cell dynamics under single-control strategies at fractional orders $\alpha = 0.7, 0.8, 0.9, 0.96, 1$ and $\beta = 0.5$. Chemotherapy (a) and immunotherapy (b) each stimulate the proliferation of normal cells under fractional-order dynamics, demonstrating that single-control strategies can enhance healthy cell populations within the modeled system.

Figure 9 displays the numerical simulations of normal cell dynamics under concurrent chemotherapy and immunotherapy across different fractional orders α. The results indicate that the combined treatment strategy effectively enhances the proliferation of normal cells compared to scenarios where controls are absent or applied individually. The synergy between chemotherapy and immunotherapy contributes to the maintenance and recovery of healthy cell populations, illustrating the therapeutic advantage of combined strategies under fractional-order dynamics in preserving normal tissue during cancer treatment.

Figure 10 presents the numerical simulations of IL-2 dynamics under single-control strategies across various fractional orders α. In Figure 10(a), immunotherapy is applied, leading to an increase in IL-2 levels over time, which reflects the immune system's activation in response to treatment. In contrast, Figure 10(b) shows chemotherapy alone maintaining lower IL-2 dynamics, indicating limited immune activation under chemotherapy-only scenarios. These results emphasize the critical role of immunotherapy in enhancing immune system activity through IL-2 signaling while illustrating the differing impacts of control strategies on immune modulation within the fractional-order tumor-immune model.

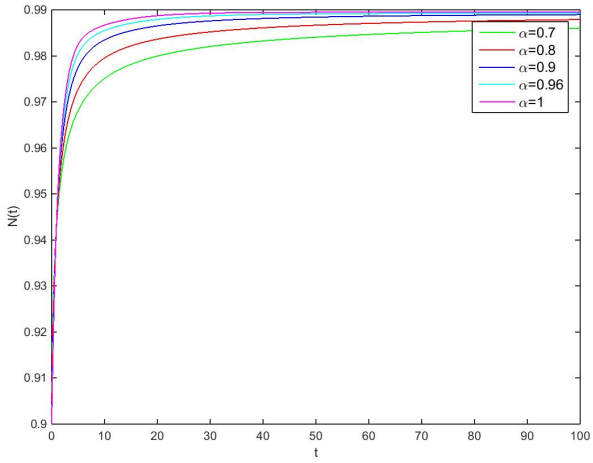

Figure 9. Dynamics of normal cells under concurrent chemotherapy and immunotherapy across fractional orders $\alpha = 0.7, 0.8, 0.9, 0.96, 1$ and $\beta = 0.5$. The combined treatment promotes normal cell proliferation more effectively than single-control strategies, demonstrating the synergistic benefit of combined chemo-immunotherapy.

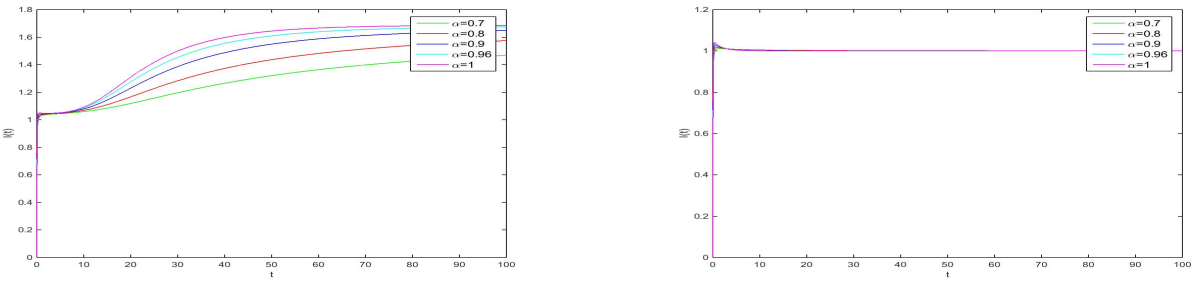

(a) IL-2 without chemotherapy (immunotherapy applied) **(b)** IL-2 without immunotherapy (chemotherapy applied)

Figure 10. Dynamics of Interleukin-2 (IL-2) under single-control strategies at fractional orders $\alpha = 0.7, 0.8, 0.9, 0.96, 1$ and $\beta = 0.5$. Immunotherapy (a) enhances IL-2 levels, while chemotherapy (b) maintains lower IL-2 dynamics, highlighting the influence of different control strategies on immune signaling.

Figure 11 presents the numerical simulations of IL-2 dynamics under immunotherapy across various fractional orders α. The results demonstrate that immunotherapy effectively increases IL-2 concentrations within the system, indicating the stimulation and activation of the immune response. This behavior highlights the crucial role of immunotherapy in promoting immune signaling pathways, which assist in the suppression of tumor cells within the fractional-order tumor-immune framework.

Figure 12 shows the numerical simulations of the chemotherapy drug dosage administered to the patient across different fractional orders α. In Figure 12(a), chemotherapy is applied without immunotherapy, while Figure 12(b) represents chemotherapy administered in conjunction with immunotherapy. The simulations illustrate the optimal dosage profiles required to effectively reduce tumor cell populations while simultaneously promoting the growth and maintenance of normal cells. The results confirm that chemotherapy drugs are potent, exerting significant impacts on both tumor and

normal cells. Through this analysis, valuable insights have been gained regarding the precise dosage strategies for managing chemotherapy during treatment, demonstrating the effectiveness of combined chemo-immunotherapy in achieving tumor reduction while preserving healthy tissue under fractional-order dynamics.

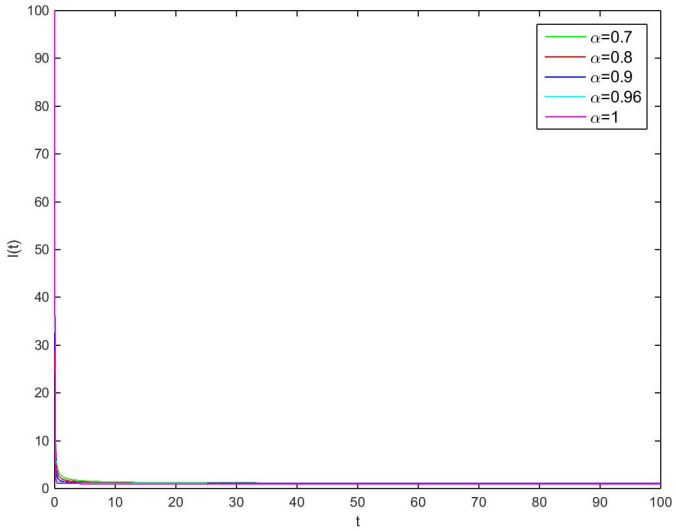

Figure 11. Dynamics of IL-2 under immunotherapy across fractional orders $\alpha = 0.7, 0.8, 0.9, 0.96, 1$ and $\beta = 0.5$. Immunotherapy effectively enhances IL-2 levels, reflecting the activation of immune responses under treatment.

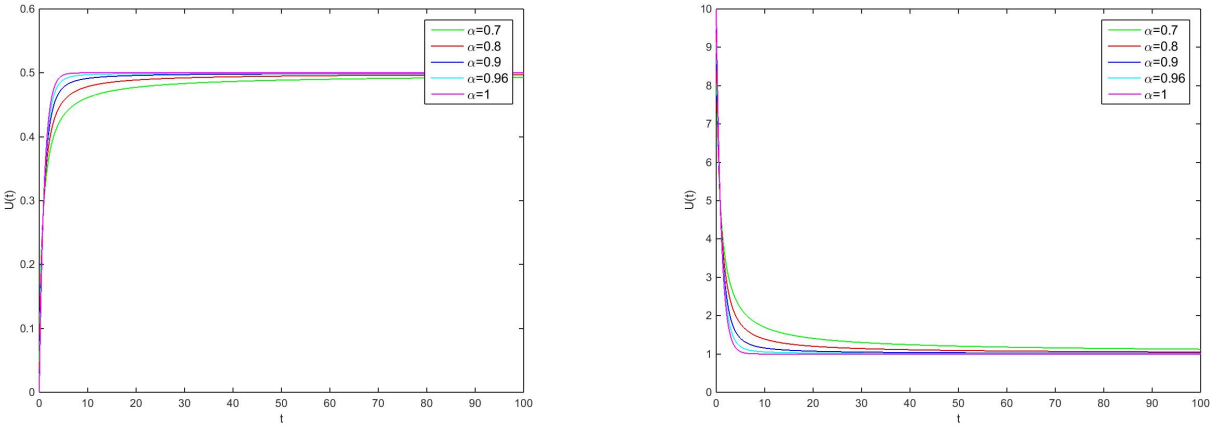

(a) Chemotherapy dosage without immunotherapy **(b)** Chemotherapy dosage with immunotherapy

Figure 12. Dynamics of chemotherapy drug dosage across fractional orders $\alpha = 0.7, 0.8, 0.9, 0.96, 1$ and $\beta = 0.5$ under (a) chemotherapy without immunotherapy and (b) chemotherapy with immunotherapy. These profiles illustrate the control strategies required to reduce tumor burden while preserving normal cell populations.

Observation of the model

- Fractional-order dynamics reflect memory effects: The model captures the memory and hereditary properties inherent in tumor-immune system interactions through fractional-order derivatives. Lower fractional orders ($\alpha = 0.7, 0.8$) exhibit slower system responses, while higher orders ($\alpha = 0.96, 1$ and $\beta = 0.5$) show faster immune and drug dynamics.
- Tumor cell behavior: Without control, tumor cells proliferate rapidly across all α values, but growth rates vary with the fractional order. Chemotherapy or immunotherapy alone can reduce tumor growth but cannot fully eradicate the tumor population. Combined chemo-immunotherapy significantly reduces tumor size, indicating a synergistic effect under fractional-order dynamics.
- Effector cell dynamics: Effector cells initially increase in response to tumor presence but plateau without control due to immune exhaustion. Immunotherapy boosts effector cell counts, while chemotherapy indirectly aids by reducing tumor burden. Combined control yields sustained effector cell activation, supporting prolonged immune response.
- Normal cell preservation: Without treatment, normal cells decline due to tumor competition and immune suppression. Immunotherapy helps maintain normal cell levels, while chemotherapy alone may slightly affect them. Combined treatment promotes normal cell proliferation while reducing tumor size, optimizing patient outcomes.
- IL-2 concentration: IL-2 levels remain low without immunotherapy. Immunotherapy significantly increases IL-2, enhancing immune-mediated tumor suppression.
- Chemotherapy dosage profile: The control strategy determines time-dependent optimal dosages to minimize tumor cells while avoiding excessive toxicity. Combined therapy requires less frequent high doses due to immunotherapy support, ensuring effective treatment with reduced side effects.
- Overall insight: The model confirms that combined fractional-order chemo-immunotherapy is more effective than single-control strategies. The system's dynamics under different α values guide personalized treatment design, emphasizing the importance of fractional modeling in capturing realistic biological behavior in cancer therapy.

7. Conclusions

In this study, we developed a fractional-order mathematical model describing the interactions between the immune system and tumor cells under an immuno-chemotherapy treatment framework, formulated as an optimal control problem using FDEs. By applying Pontryagin's Maximum Principle to the adjoint system, we derived the necessary conditions for the optimal control strategy that minimizes tumor burden while enhancing effector cell and IL-2 concentrations and reducing the side effects associated with chemotherapy. The existence of an optimal control was established, and the optimality conditions were rigorously derived using a Pontryagin-type Minimum Principle. Numerical simulations conducted over a 100-day treatment horizon demonstrated the effectiveness of the proposed chemo-immunotherapy regimen in significantly reducing the tumor size while promoting the proliferation of effector and normal cells.

Future research will focus on conducting a comprehensive sensitivity analysis to identify the key parameters influencing the system's dynamics and the effectiveness of the treatment strategy. Investigating the stability and robustness of the tumor-free equilibrium under small parameter

variations will provide valuable insights for clinical implementation. Additionally, exploring alternative and combination control strategies, such as integrating chemotherapy with different immunotherapy protocols, may yield improved treatment outcomes and enhance the practical applicability of fractional-order models in personalized cancer therapy.

Author contributions

K. Ramalakshmi: Formal analysis, software, methodology; B. Sundara Vadivoo: Formal analysis, software, methodology; Dilber Uzun Ozsahin: Investigation, validation, methodology; Hijaz Ahmad: Investigation, writing-review and editing, supervision; Taha Radwan: Investigation, data curation, resources, writing-review and editing. All authors have read and approved the final version of the manuscript for publication.

Use of Generative-AI tools declaration

The authors declare they have not used Artificial Intelligence (AI) tools in the creation of this article.

Acknowledgments

The researchers would like to thank the Deanship of Graduate Studies and Scientific Research at Qassim University for financial support (QU-APC-2025).

Conflict of interest

All authors declare no conflict of interest in this paper.

References

1. G. K. Antony, A. Z. Dudek, Interleukin 2 in cancer therapy, *Curr. Med. Chem.*, **17** (2010), 3297–3302. http://dx.doi/10.2174/092986710793176410
2. S. Banerje, Immunotherapy with interleukin-2: A study based on mathematical modeling, *Int. J. Ap. Mat. Com.-Pol.*, **18** (2008), 389–398. http://dx.doi/10.2478/v10006-008-0035-6
3. V. A. Kuznetsov, I. A. Makalkin, M. A. Taylor, A. S. Perelson, Nonlinear dynamics of immunogenic tumors: Parameter estimation and global bifurcation analysis, *B. Math. Biol.*, **56** (1994), 295–321. https://doi.org/10.1016/S0092-8240(05)80260-5
4. L. G. D. Pillis, K. R. Fister, W. Gu, T. Head, K. Maples, T. Neal, et al., Optimal control of mixed immunotherapy and chemotherapy of tumors, *J. Biol. Syst.*, **16** (2008), 51–80. https://doi.org/10.1142/S0218339008002435
5. P. Khalili, R. Vatankhah, Optimal control design for drug delivery of immunotherapy in chemoimmunotherapy treatment, *Comput. Meth. Prog. Bio.*, **229** (2023), 107248. https://doi.org/10.1016/j.cmpb.2022.107248

6. K. Ramalakshmi, B. Sundaravadivoo, Necessary conditions for Ψ-Hilfer fractional optimal control problems and Ψ-Hilfer two-step Lagrange interpolation polynomial, *Int. J. Dynam. Control*, **12** (2024), 42–55. https://doi.org/10.1007/s40435-023-01342-y
7. D. Baleanu, A. Jajarmi, S. S. Sajjadi, D. Mozyrska, A new fractional model and optimal control of a tumor-immune surveillance with non-singular derivative operator, *Chaos*, **29** (2019), 083127. https://doi.org/10.1063/1.5096159
8. K. J. Mahasa, R. Ouifki, A. Eladdadi, L. Pillis, Mathematical model of tumor-immune surveillance, *J. Theor. Biol.*, **404** (2016), 312–330. https://doi.org/10.1016/j.jtbi.2016.06.012
9. D. Kirschner, J. Panetta, Modeling immunotherapy of the tumor-immune interaction, *J. Math. Biol.*, **37** (1998), 235–252. https://doi.org/10.1007/s002850050127
10. A. A. Kilbas, H. M. Srivastava, J. J. Trujillo, *Theory and applications of fractional differential equations*, North-Holland Mathematics Studies: Elsevier, 2006. http://dx.doi/10.1016/S0304-0208(06)80001-0
11. O. P. Agrawal, General formulation for the numerical solution of optimal control problems, *Int. J. Control*, **50** (1989), 627–638. https://doi.org/10.1080/00207178908953385
12. F. A. Rihan, D. H. Abdelrahman, F. A. Maskari, F. Ibrahim, M. A. Abdeen, Delay differential model for tumour-immune response with chemoimmunotherapy and optimal control, *Comput. Math. Method. M.*, **2014** (2014), 982978. https://doi.org/10.1155/2014/982978
13. K. Shahzadi, A. Tariq, U. Ali, M. A. Khan, An efficient analytical solution for fractional order cancer model; Laplace transformation, *Global J. Sci.*, **1** (2024), 1–11. https://doi.org/10.48165/gjs.2024.1201
14. H. Schattler, U. Ledzewicz, *Optimal control for mathematical models of cancer therapies*, New York: Springer, 2015. https://doi.org/10.1007/978-1-4939-2972-6
15. H. Gu, J. J. Trujillo, Existence of mild solution for evolution equation with Hilfer fractional derivative, *Appl. Math. Comput.*, **257** (2015), 344–354. https://doi.org/10.1016/j.amc.2014.10.083
16. M. M. Raja, V. Vijayakumar, K. C. Veluvolu, Improved order in Hilfer fractional differential systems: Solvability and optimal control problem for hemivariational inequalities, *Chaos Soliton. Fract.*, **188** (2024), 115558. https://doi.org/10.1016/j.chaos.2024.115558
17. M. M. Raja, V. Vijayakumar, A. Shukla, K. S. Nisar, N. Sakthivel, K. Kaliraj, Optimal control and approximate controllability for fractional integrodifferential evolution equations with infinite delay of order r∈(1, 2), *Optim. Contr. Appl. Met.*, **43** (2022), 996–1019. https://doi.org/10.1002/oca.2867

AIMS Press